A life-history allele of large effect shortens developmental time in a wild insect population

Cheng, S.; Jacobs, C.G.; Mogollón Pérez, E.A.; Chen, D.; Sanden, J.T. van de; Bretscher, K.M.; ... ; Zee, M. van der

nature ecology & evolution

Article

https://doi.org/10.1038/s41559-023-02246-y

A life-history allele of large effect shortens developmental time in a wild insect population

Received: 26 April 2023

Accepted: 4 October 2023

Published online: 13 November 2023

Check for updates

Shixiong Cheng[1], Chris G. C. Jacobs[1], Elisa A. Mogollón Pérez[1,4], Daipeng Chen[2], Joep T. van de Sanden[1,5], Kevin M. Bretscher[1], Femke Verweij[1], Jelle S. Bosman[1], Amke Hackmann[1], Roeland M. H. Merks[1,2], Joost van den Heuvel[3] & Maurijn van der Zee[1]

Developmental time is a key life-history trait with large effects on Darwinian fitness. In many insects, developmental time is currently under strong selection to minimize ecological mismatches in seasonal timing induced by climate change. The genetic basis of responses to such selection, however, is poorly understood. To address this problem, we set up a long-term evolve-and-resequence experiment in the beetle *Tribolium castaneum* and selected replicate, outbred populations for fast or slow embryonic development. The response to this selection was substantial and embryonic developmental timing of the selection lines started to diverge during dorsal closure. Pooled whole-genome resequencing, gene expression analysis and an RNAi screen pinpoint a 222 bp deletion containing binding sites for Broad and Tramtrack upstream of the ecdysone degrading enzyme Cyp18a1 as a main target of selection. Using CRISPR/Cas9 to reconstruct this allele in the homogenous genetic background of a laboratory strain, we unravel how this single deletion advances the embryonic ecdysone peak inducing dorsal closure and show that this allele accelerates larval development but causes a trade-off with fecundity. Our study uncovers a life-history allele of large effect and reveals the evolvability of developmental time in a natural insect population.

The timing of developmental processes is crucial in evolution and development[1,2]. The duration of development, developmental time (DT), determines traits such as age and size at reproduction[3,4], and is thus a critical life-history trait with large effects on biological fitness. Such life-history traits are expected to be highly optimized by stabilizing selection[5] and buffered ('canalized') against perturbations[6,7]. In insects, life histories are well synchronized with seasonal availability of host plants or prey. However, when species respond differently to global warming, ecological mismatches in seasonal timing may occur[8–10]. These 'phenological mismatches' currently exert strong selection on insect DT[11,12]. A striking example of a response to such selection is the genetic adaptation of embryonic DT in the winter moth *Operophtera brumata* to synchronize the hatching of caterpillars from the egg with oak tree leaf-out in spring[13]. Yet, the genetic basis of such adaptation in DT is largely unknown[14,15].

Surprisingly little is known about the genetics of DT in insects. An insertional mutagenesis screen in *Drosophila* revealed 102 genes affecting DT[16]. It is unclear, however, whether any relevant natural

[1]Institute of Biology, Leiden University, Leiden, the Netherlands. [2]Mathematical Institute, Leiden University, Leiden, the Netherlands. [3]Laboratory of Genetics, Wageningen University and Research, Wageningen, the Netherlands. [4]Present address: Faculty of Biology, Ludwig-Maximilians-Universität München, Planegg-Martinsried, Germany. [5]Present address: Department of Radiology and Nuclear Medicine, Erasmus MC, Rotterdam, the Netherlands. e-mail: m.van.der.zee@biology.leidenuniv.nl

https://doi.org/10.1038/s41559-023-02246-y

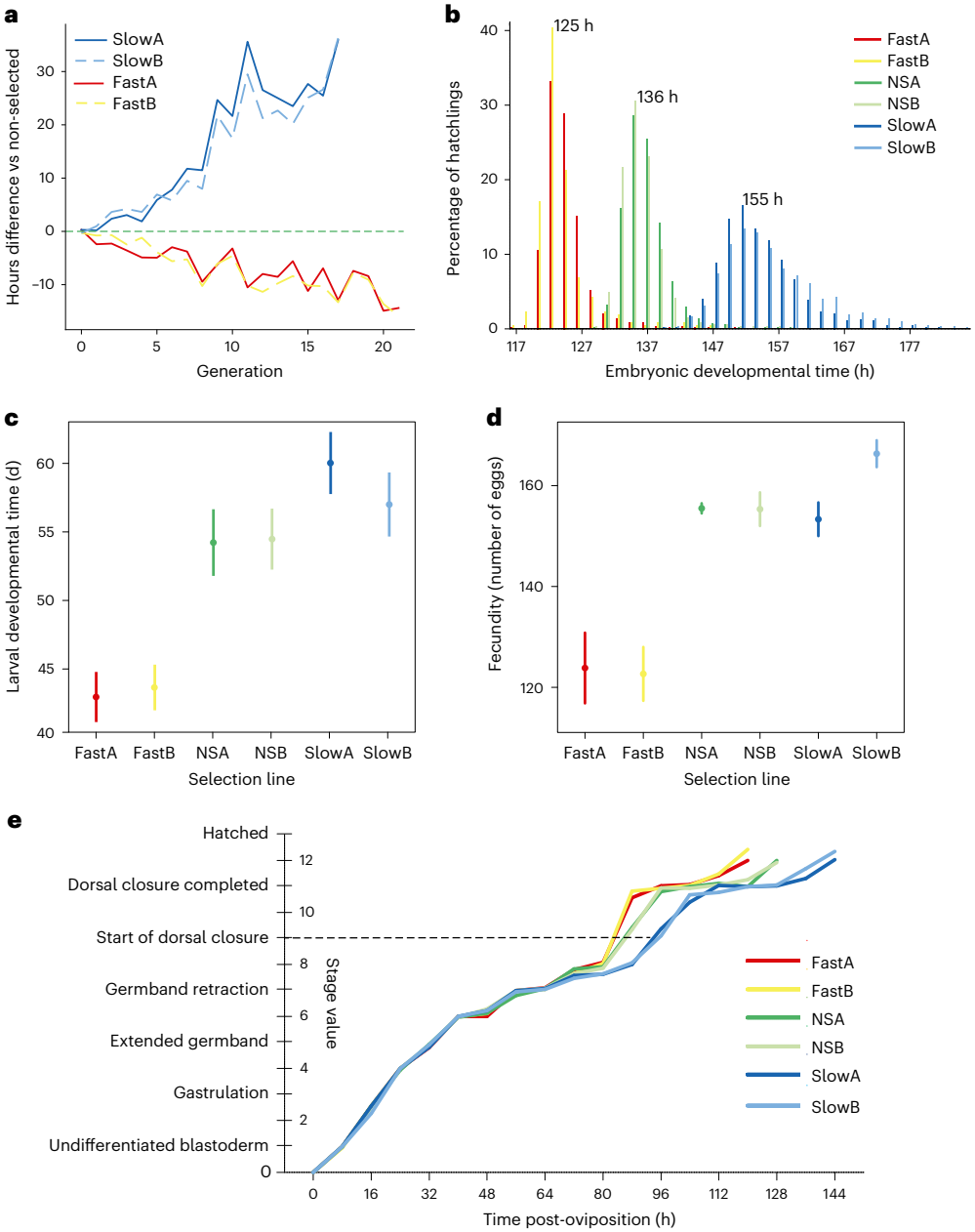

Fig. 1 | Life-history traits of the selection lines. a, Average embryonic developmental time in the slow and fast lines (hours from egg laying to hatching) over the 21 generations of selection (17 for the slow lines), zeroed against the non-selected (NS) lines. **b**, Distribution of developmental times at 25 °C (hours from egg laying to hatching) in each line after selection (see **a**), followed by 10 generations without selection. Averages of the A and B lines together are indicated above the histograms (n = 1,357 for FastA, 263 for FastB, 1,778 for NSA, 1,608 for NSB, 1,257 for SlowA and 1,094 for SlowB). **c**, Larval developmental time (days from hatching to pupation; means ± 2 × s.e.m.; n = 48 for each selection line). Selection regime had an effect (χ^2 = 23.66; d.f. = 2; P = 0.000007): larvae from fast lines developed significantly faster (χ^2 = 17.65; d.f. = 1; P = 0.00003) and larvae from slow lines developed significantly slower (χ^2 = 15.64; d.f. = 1; P = 0.00007) than larvae from non-selected lines. Sex had no effect (χ^2 = 0.15; d.f. = 1; P = 0.698). **d**, Fecundity expressed as number of eggs laid by 50 females in 4 h (means ± 2 × s.e.m). Selection regime had an effect (χ^2 = 11.78; d.f. = 2; P = 0.003): females from fast lines laid fewer eggs than those from non-selected lines (χ^2 = 11.56; d.f. = 1; P = 0.0007). **e**, Developmental stages during embryonic developmental time (hours after egg laying) of the selection lines (stage values defined in Extended Data Fig. 2). Start of dorsal closure is the first stage at which a difference in timing can be detected among the selection lines (dashed line).

variation in these genes exists in nature. Some knowledge on naturally occurring genetic variation for DT in *Drosophila melanogaster* comes from Genetic Reference Panel strains and studies on clines[17,18]. Notably, responses to artificial selection on DT have been demonstrated in *Drosophila*[19–23] and other insects[24–26]. However, all these studies have focused on larval, pupal or total DT. Artificial selection experiments on embryonic DT have been rare[27,28], or yielded no response[29]. Moreover, the genetic basis underlying the responses has not been investigated.

To investigate the evolvability and genetic basis of embryonic DT in insects, we apply a long-term evolve-and-resequence approach[30] to a wild population of the tractable model insect *Tribolium castaneum*[31,32].

Early dorsal closure but reduced fecundity in the fast lines

From an outbred population (see Methods), we collected a 2 h egg lay and selected the earliest-hatching half of the larvae for a fast line (FastA)

https://doi.org/10.1038/s41559-023-02246-y

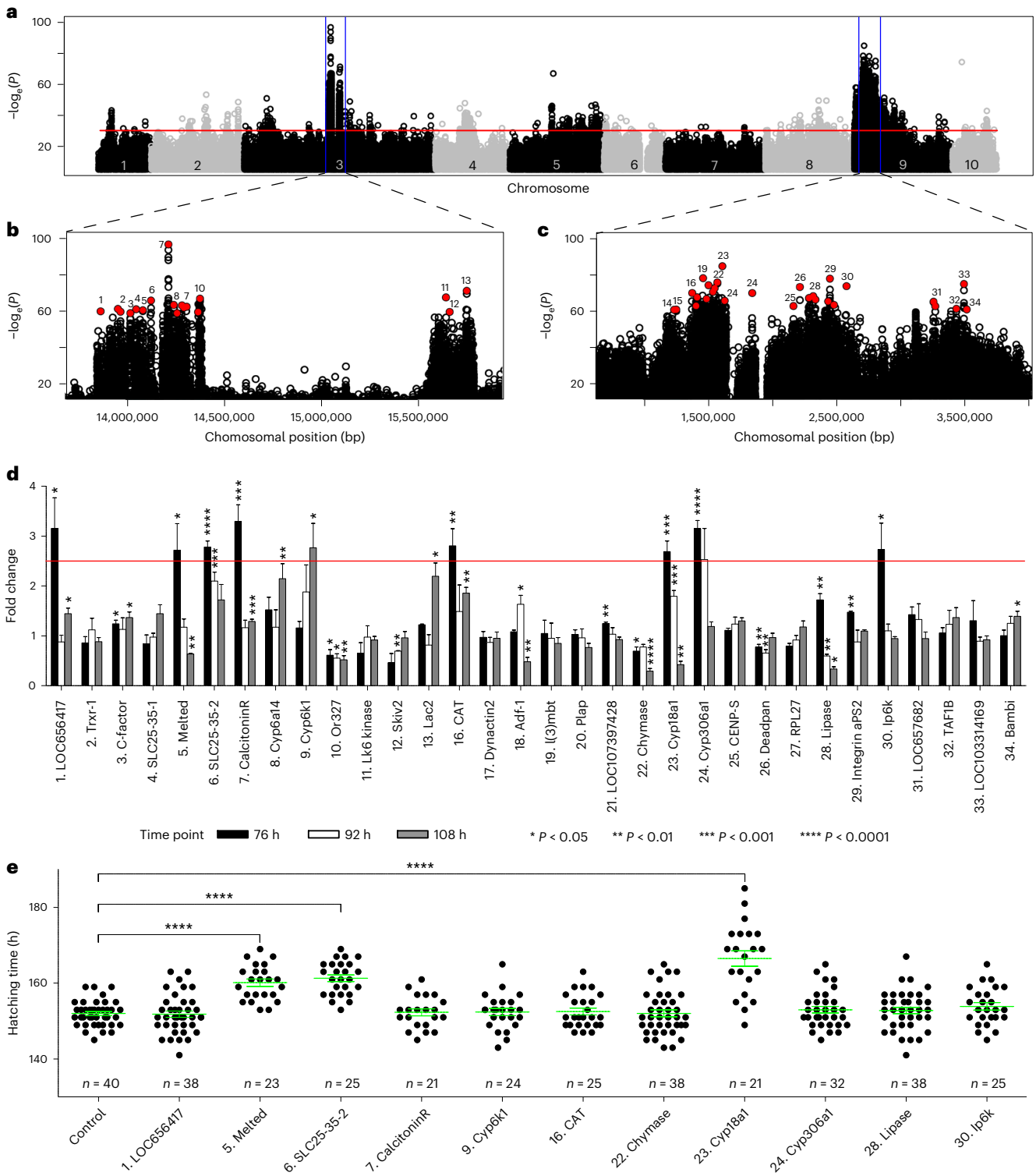

Fig. 2 | Identification of candidate genes under selection. a, *P* values of SNPs based on a GLM contrasting the fast ($n = 2$) and the non-selected ($n = 2$) lines (see Methods) along the 10 chromosomes of *T. castaneum*. Above the red line, their allele frequency difference is significant ($q < 0.01$, $-\log_e(P) > 30.2275$). **b**,**c**, *P* values of SNPs based on a GLM contrasting the fast ($n = 2$) and the non-selected ($n = 2$) lines, from 13.8–15.8 MB on chromosome 3 (**b**) and from 0.5–4 MB on chromosome 9 (**c**). Lead SNPs (see Methods) are indicated in red. Numbers refer to their associated genes. See all lead SNPs and their associated genes in Supplementary Table 1. **d**, Fold change of candidate gene expression in the fast lines compared to the non-selected lines on chromosome 3 and on chromosome 9 at timepoints 76 (black), 92 (white) and 108 (grey) h after egg laying (means ± s.e.m.). Red line indicates 2-fold higher expression in the fast lines. $^{*}P < 0.05$, $^{**}P < 0.01$, $^{***}P < 0.001$, $^{****}P < 0.0001$ (unpaired two-sided *t*-test, see Methods). For two polycystin-related genes (genes 14 and 15), we could not detect any expression. The qPCR data are based on two biological replicates (200–300 eggs) from the two fast lines (thus, $n = 4$), each measured as the average of 2 technical qPCR replicates compared to the same number of replicates from the non-selected lines (see Source Data for all 758 datapoints and 96 exact *P* values). **e**, Embryonic developmental time (hours) of eggs derived from ~50 dsRNA-injected *Tribolium* GA-1 mothers compared to eggs derived from mothers injected with a control dsRNA (see Methods). Green, mean ± s.e.m. *P* values by unpaired two-sided *t*-test: $^{****}P = 1.1 \times 10^{-8}$ for *Melted*, 2.0×10^{-11} for *SLC25-35-2* and 5.9×10^{-7} for *Cyp18a1*.

https://doi.org/10.1038/s41559-023-02246-y

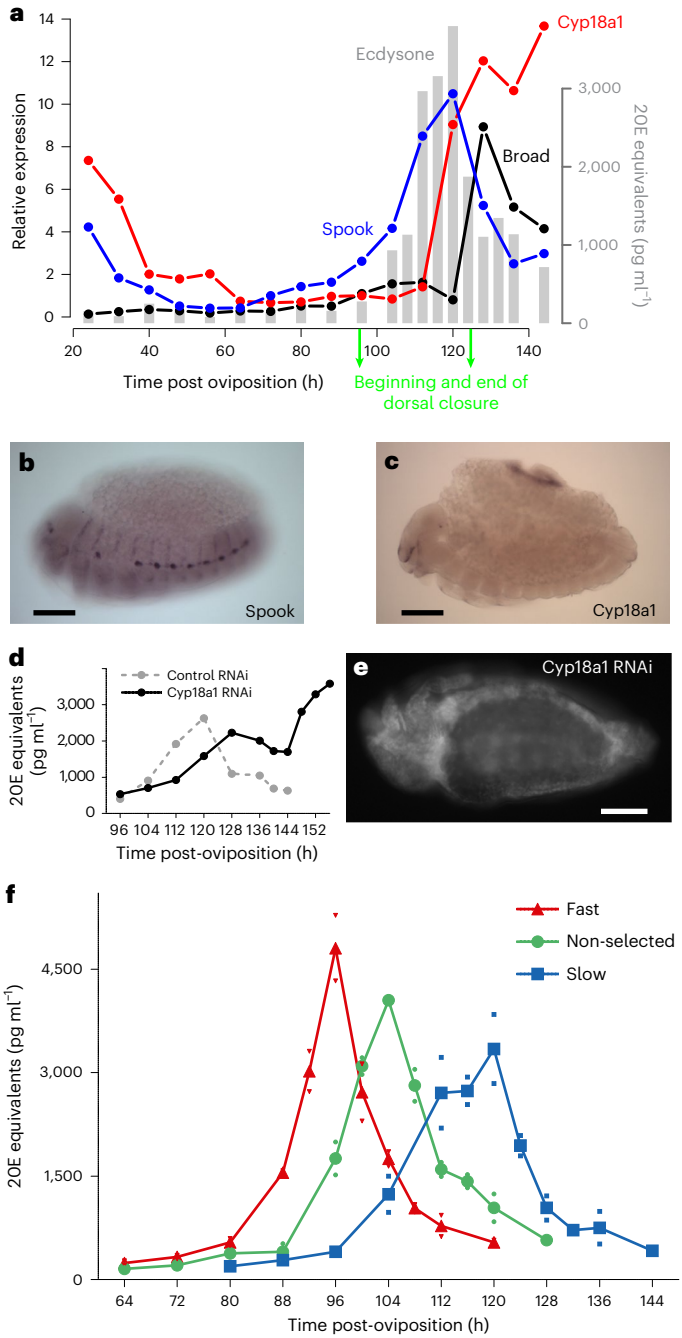

Fig. 3 | Ecdysone regulates dorsal closure. a, Ecdysone titres (grey columns, right *y* axis, means of 2 technical replicates) and relative expression of *Spook* (blue), *Broad* (black) and *Cyp18a1* (red) with respect to timepoints 72 h, 96 h and 96 h, respectively, determined by qPCR. Spook and ecdysone levels start to rise during dorsal closure (green arrows). **b**, In situ hybridization for *Spook* at the retracted germband stage. Spook is expressed in the tracheae and in stripes in the dorsal ectoderm. Representative embryo of one in situ hybridization on >25 eggs. Scale bar, 200 µm. **c**, In situ hybridization for *Cyp18a1* at the beginning of dorsal closure. *Cyp18a1* is expressed in the dorsal organ (the retracting serosa). Staining in the sticky mouthparts is an artefact. Representative embryo of one in situ hybridization on >25 eggs. Scale bar, 200 µm. **d**, Ecdysone levels in *Cyp18a1* pRNAi embyos (means of 2 technical replicates). **e**, Around one quarter of all *Cyp18a1* pRNAi embryos displays developmental arrest at the start of dorsal closure (result of one pRNAi treatment, see Extended Data Fig. 4). Scale bar, 200 µm. **f**, Ecdysteroid levels of the eggs of the selection lines. Large symbols are the means of the fast (red triangles), non-selected (green circles) and slow (blue squares) lines. Small symbols represent each biological replicate ($n = 2$), measured as the average of 2 technical replicates (see Source Data).

and the latest-hatching half for a slow line (SlowA), and repeated this for two replicate lines (FastB, SlowB). We continued selection for 21 generations in the fast lines and 17 in the slow lines while maintaining two independent egg lays without selection (NSA, NSB). The response to this selection was spectacular (Fig. 1a) and resulted in more than a day of difference in embryonic DT between the fast and the slow lines (20% of total embryonic DT; Fig. 1b). As correlated responses, larval, pupal and total DT also differentiated significantly among the selection treatments (Fig. 1c and Extended Data Fig. 1a,b). Interestingly, growth rate (mg d^{-1}) did not differentiate between the fast and slow lines (Extended Data Fig. 1c), suggesting that, predominantly, pure timing mechanisms evolved.

Classical life-history theory predicts that DT trades off with weight and fecundity, as long-developing larvae have more time to obtain resources[4,5,33,34]. Indeed, pupae and adults of the slow lines were significantly heavier than the non-selected and fast lines (Extended Data Fig. 1d,e), while early fecundity was significantly reduced in the fast lines (Fig. 1d) but not vice-versa. In contrast to *Caenorhabditis elegans* strains[35], but as in *Drosophila*[20,23], DT did not correlate with adult longevity (Extended Data Fig. 1f). To examine when, during embryonic development, responses to selection occurred, we used developmental staging (Extended Data Fig. 2) of sequential samples of the lines taken every 8 h during embryogenesis (every $n \approx 50$ embryos). The average stage values demonstrate that there is no difference in embryonic timing until the start of dorsal closure, one of the last stages of development when the lateral sides of the embryo fuse dorsally to enclose the yolk[36] (Fig. 1e). In summary, dorsal closure occurs earlier in the fast lines, which is correlated with shorter larval development and a trade-off with fecundity.

Cyp18a1 is a main target of selection

To investigate the genetic basis of this response, we performed whole-genome resequencing on pools of ~100 eggs from each selection line[37], identified single nucleotide polymorphisms (SNPs) and estimated the significance of their frequency differences among the treatments using a generalized linear model (GLM)[38]. While only 1,258 SNPs differed significantly in frequency between the slow and non-selected lines ($q < 0.01$, Extended Data Fig. 3), 8,469 SNPs do so between the fast and non-selected lines (Fig. 2a). We focused on these latter SNPs. Most of the highest SNPs are located on chromosome 3 (between position 13.8–15.8 MB), or on chromosome 9 (between 0.5–4 MB) (Fig. 2a). In these areas, we defined 46 lead SNPs (SNPs that do not have any higher SNP within 10 kb distance) on the basis of significance and size of their allele frequency difference, and associated them with 34 candidate genes (numbered in Fig. 2b,c; see Supplementary Table 1). None of these SNPs is located in protein coding sequences, except for SNP 19 and 25 which are synonymous substitutions. Therefore, we subsequently investigated differential expression of the 34 candidate genes between the fast and non-selected lines before (76 h), during (92 h) and after (108 h) dorsal closure. Twenty-one genes showed significant differential expression on at least one of these timepoints, including 11 genes that showed a larger than 2.5-fold change (that is, higher than 2.5- or lower than 0.4-fold expression) (Fig. 2d). Finally, we performed RNA interference (RNAi) against all these 11 candidate genes to investigate their influence on DT. RNAi against 3 genes led to a significant developmental delay (Fig. 2e): *Melted, SLC25-35-2* and *Cyp18a1*. *Melted* and *SLC25-35-2* map on chromosome 3 to a region of major chromosomal rearrangements, which we could not reconstruct using Illumina short reads. We therefore focused on *Cyp18a1* (gene 23), the gene with the largest RNAi effect on DT (Fig. 2e) and the gene identified by the highest SNP on chromosome 9 (at position 1,613,665).

An embryonic ecdysone pulse starts dorsal closure

Cyp18a1 encodes a cytochrome P450 enzyme that degrades active ecdysone (20E) by 26-hydroxylation[39,40]. The steroid hormone 20E

https://doi.org/10.1038/s41559-023-02246-y

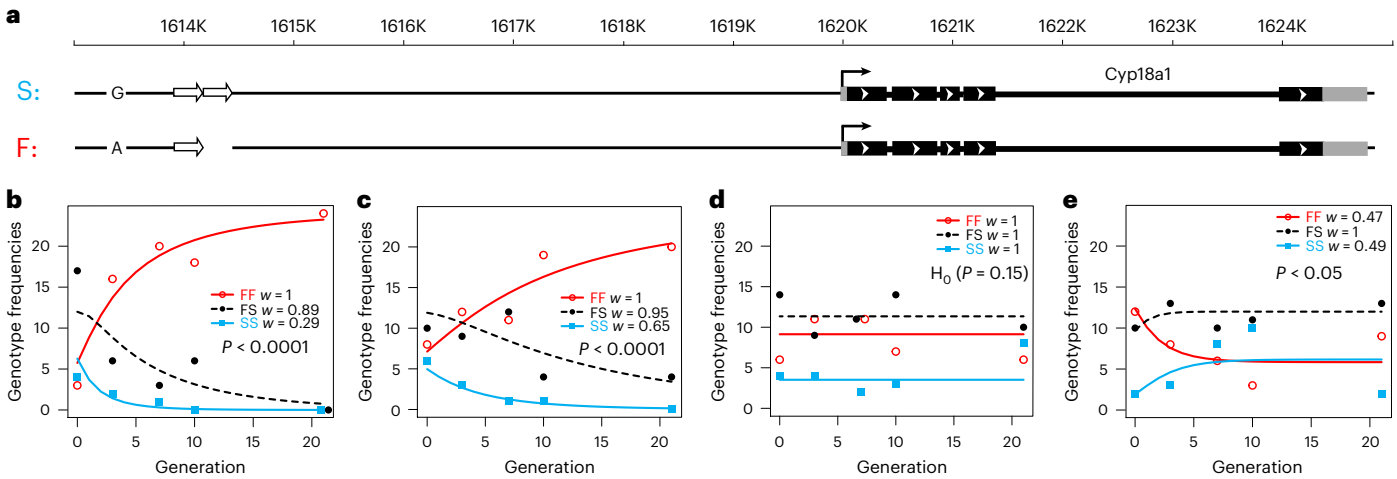

Fig. 4 | Selection for the F allele in the fast lines. a, Schematic drawing of the S and F allele on chromosome 9. The reference allele S contains two repeated elements of 222 bp (open arrows) ~6 kb upstream of the *Cyp18a1* transcription start site and 300 bp downstream of the lead SNP for *Cyp18a1* (G/A at position 1,613,665). In the alternative F allele, one of these elements is deleted. **b**–**e**, In 24 stored beetles of each selection line, we determined the frequencies of FF (red circles), FS (black circles) and SS (blue squares) individuals in generations 0, 3, 7, 10 and 21. We fitted starting allele frequency and relative fitness models to these observations, taking equal fitnesses as null hypothesis (H_0). Best-fit relative fitness values (w) are indicated next to the genotypes. P values indicate how significantly the permutated model fits the data compared to the equal fitness model (χ^2 test, d.f. = 2, see Methods). We find strong evidence for positive selection on the F allele in the fast lines ($P = 6.3 \times 10^{-11}$ in FastA, $P = 1.3 \times 10^{-5}$ in FastB) (**b**,**c**). We detect no selection in the non-selected A line ($P = 0.15$) (**d**) and non-directional selection in the non-selected B line (weak evidence for heterozygote advantage, $P = 0.03$) (**e**).

(hereafter, 'ecdysone') is crucial in controlling developmental timing, such as moulting and metamorphosis, and is synthesized by other cytochrome P450 enzymes collectively called the Halloween genes[41,42]. An ecdysone peak during *Drosophila* embryogenesis[43,44] was recently shown to regulate dorsal closure[45], and ecdysone can end diapause to start katatrepsis in *Locusta migratoria* embryos[46]. Hence, we measured ecdysone levels and expression of the Halloween gene *Spook*, the ecdysone target gene *Broad*[42] and *Cyp18a1*, during embryogenesis of the *Tribolium* laboratory strain Georgia (GA-1). Indeed, *Spook* mRNA and ecdysone levels start to increase at the beginning of dorsal closure and peak towards the end (Fig. 3a). 20E levels decrease again when *Cyp18a1* expression is high and *Broad* expression follows ecdysone levels (Fig. 3a). In situ hybridizations during dorsal closure stages show that *Spook* is expressed in the dorsal ectoderm already before dorsal closure (Fig. 3b) and that during dorsal closure, *Cyp18a1* starts to be expressed in the dorsal organ formed by the contracting serosa[36] (Fig. 3c). Parental RNAi against *Spook* or the ecdysone receptors leads to sterility, but *Cyp18a1* RNAi in GA-1 yields eggs in which ecdysone levels continue to increase (Fig. 3d). This demonstrates that *Cyp18a1* also degrades active ecdysone in *Tribolium*. Around one quarter of the eggs develop with a strong delay (Fig. 2e), but two-thirds show developmental arrests, most of which take place at dorsal closure (Fig. 3e and Extended Data Fig. 4). From these data, we conclude that a pulse of ecdysone is required to induce dorsal closure and that continuous high levels are not sufficient, as also shown for the juvenile–adult transition[40]. The timing of the ecdysone peaks differs accordingly among our *Tribolium* selection lines (Figs. 3f and 1e).

The fast allele is an allele of large effect

At position 1,613,941 on chromosome 9, less than 300 bp downstream of the *Cyp18a1* lead SNP and ~6 kb upstream of the *Cyp18a1* transcription start site, a 444 bp sequence starts that consists of two repeated 222 bp elements (arrows in Fig. 4a, S allele). Reassembly of the pooled resequencing reads mapping to this region indicates the presence of an alternative allele in which one of these elements is deleted. We call this the F allele (Fig. 4a). Allele-specific read counts indicate that its frequency is 1 in the fast lines, 0 in the slow lines, and 0.15 and 0.16 in the two non-selected lines (Supplementary Table 2). Sanger sequencing of cloned PCR products obtained from fast, non-selected and slow beetles confirmed the presence of such alleles (Supplementary Data 1). Using PCR, we determined that both alleles are present in the original wild population of *Tribolium castaneum* that was used to set up our outbred starting population (Extended Data Fig. 5). Most importantly, we determined genotype frequencies in individual beetles of generations 0, 3, 7, 10 and 21 stored during the selection experiment. Population genetic modelling detects no or non-directional selection for the F allele in the non-selected lines (Fig. 4d,e), but strong positive selection on the F allele in the fast lines (Fig. 4b,c).

Genotyping the 64 first and 64 last hatching larvae out of ~2,000 eggs from the non-selected (NS) lines shows that the F allele is significantly associated with fast development in the NSB line (Supplementary Table 3). However, this was not significant in the NSA line (Supplementary Table 3), suggesting that genetic background and other alleles are also relevant. To study the F allele in isolation, we applied CRISPR/Cas9 using a single guide RNA (gRNA) to reconstruct this deletion in the homogeneous genetic background of the inbred GA-1 strain homozygous for the repeat (Fig. 5a). Strikingly, embryos of the homozygous CRISPR/Cas9 line developed 5 h faster than embryos from GA-1 (Fig. 5b), which is half of the time difference between the fast and non-selected lines (Fig. 1b). As a consequence[4,5,33,34], fecundity was also reduced in the CRISPR/Cas9 line (Fig. 5c). Consistent with the faster development, the embryonic ecdysone peak occurred earlier in the CRISPR line than in GA-1 (Fig. 5d). Surprisingly, however, *Cyp18a1* expression started to rise later in the CRISPR line (Fig. 5e). We address this in the next section.

Finally, we crossed our CRISPR line with the nGFP line[47] and live imaged their heterozygous offspring (Supplementary Video 1). Imaging analysis shows that the retracted germband stage (the stage preceding the start of dorsal closure) occurs at the same time as in heterozygous nGPP/GA-1 offspring (Fig. 5f), but that the interval to the start of dorsal closure is significantly shorter in the nGFP/CRISPR offspring (Fig. 5g). Only this start is earlier; the duration of the dorsal closure process itself is not shorter (Fig. 5h). Taken together, our data show that this single 222 bp deletion advances the embryonic ecdysone peak and dorsal closure, and causes a trade-off with fecundity.

https://doi.org/10.1038/s41559-023-02246-y

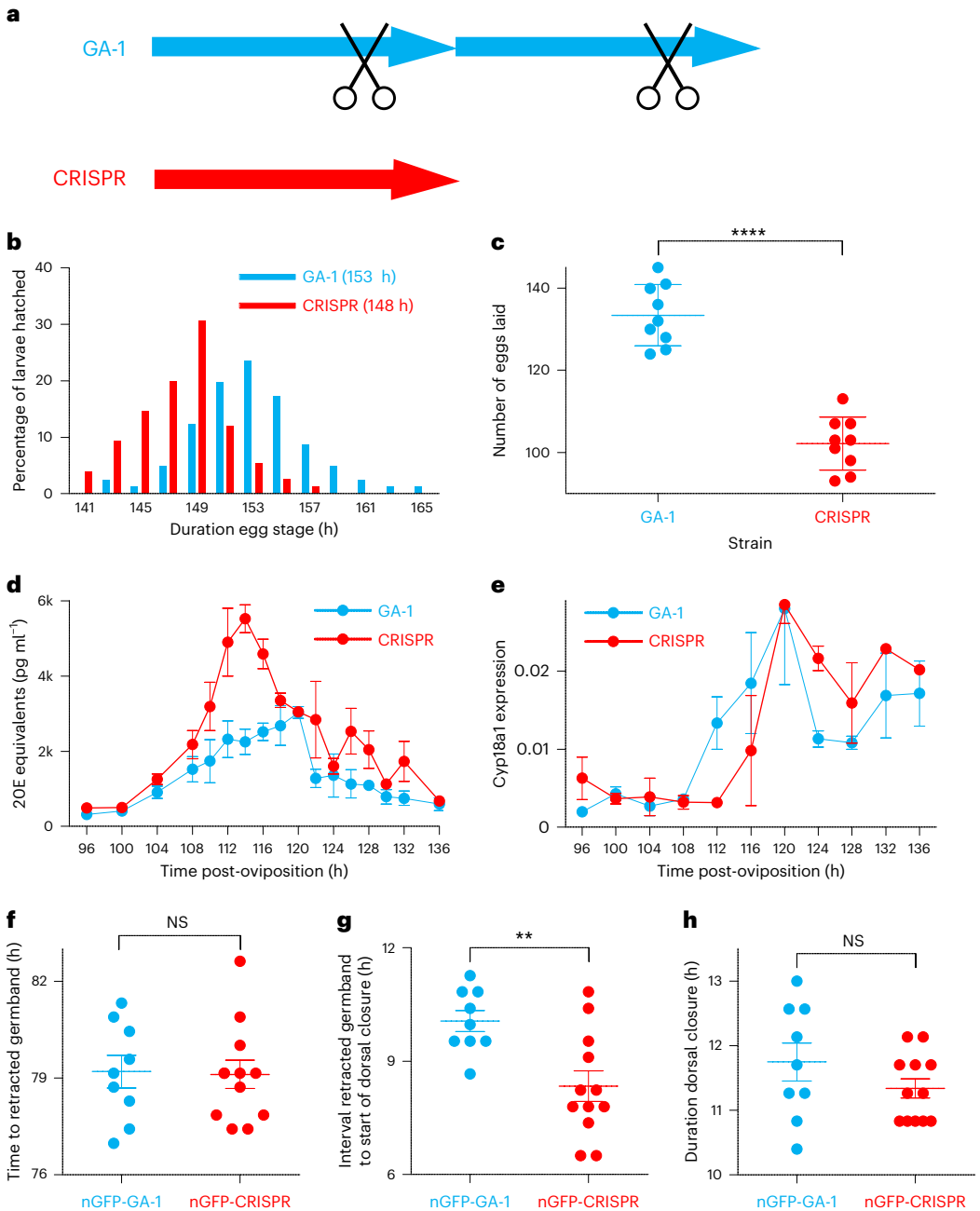

Fig. 5 | CRISPR/Cas9 re-creation of the F allele. a, Schematic drawing of the CRISPR/Cas9 approach: using a single guide (scissors) targeting the repeat (arrows) in GA-1, we re-created the deletion (CRISPR, red) in the homogeneous genetic background. **b**, Distribution of embryonic developmental time (egg laying to hatching) of GA-1 eggs (blue) and eggs of the homozygous CRISPR line (red). Average DT is 153 h for GA-1 ($n = 81$) and 148 h for CRISPR ($n = 75$). **c**, Fecundity expressed as number of eggs laid by 50 females in 4 h for GA-1 (blue) and CRISPR (red) lines. Fecundity is significantly reduced in the CRISPR line (means ± s.e.m., unpaired two-sided *t*-test, $P = 5.9 \times 10^{-5}$). **d**, Ecdysteroid levels (pg ml^{-1}) in eggs of the GA-1 (blue) and CRISPR (red) lines (means ± s.e.m.). The 20E peak is higher and earlier in the CRISPR line (3 biological replicates measured in 2 technical replicates). **e**, *Cyp18a1* expression in GA-1 (blue) and CRISPR (red) lines relative to expression of the reference gene *RPL13a* (means ± s.e.m.). *Cyp18a1* starts to rise later in the CRISPR line. **f**–**h**, Live imaging analysis of GA-1/nGFP (blue, $n = 9$) and CRISPR/nGFP (red, $n = 12$) heterozygous embryos (means ± s.e.m.). Stages are defined in Extended Data Fig. 2. **f**, Times from egg laying to the completely retracted germband are not significantly different (unpaired two-sided *t*-test, $P = 0.90$). **g**, The intervals between the completely retracted germband and the onset of dorsal closure (membrane rupture, dorsal organ formation) are significantly shorter in CRISPR/nGFP heterozygotes (unpaired two-sided *t*-test, $P = 0.0038$). **h**, Durations of dorsal closure (interval from start of dorsal closure to complete dorsal closure) are not significantly different (unpaired two-sided *t*-test, $P = 0.196$).

The fast allele makes *Cyp18a1* less sensitive to ecdysone

We reasoned that the deletion may be located in a *cis*-regulatory element affecting *Cyp18a1* expression. Indeed, FIMO[48] predicts, in the whole upstream 8 kb intergenic region, only a single high-affinity binding site for Broad (Z4) ($P < 1 \times 10^{-5}$) and a single binding site for Tramtrack ($P < 1 \times 10^{-4}$) right in the element, thus repeated in the S allele, immediately followed by an ecdysone receptor/USP binding site (Fig. 6a and Supplementary Data 2). The transcription factor Broad is critical for the appropriate upregulation of ecdysone-inducible genes[49].

https://doi.org/10.1038/s41559-023-02246-y

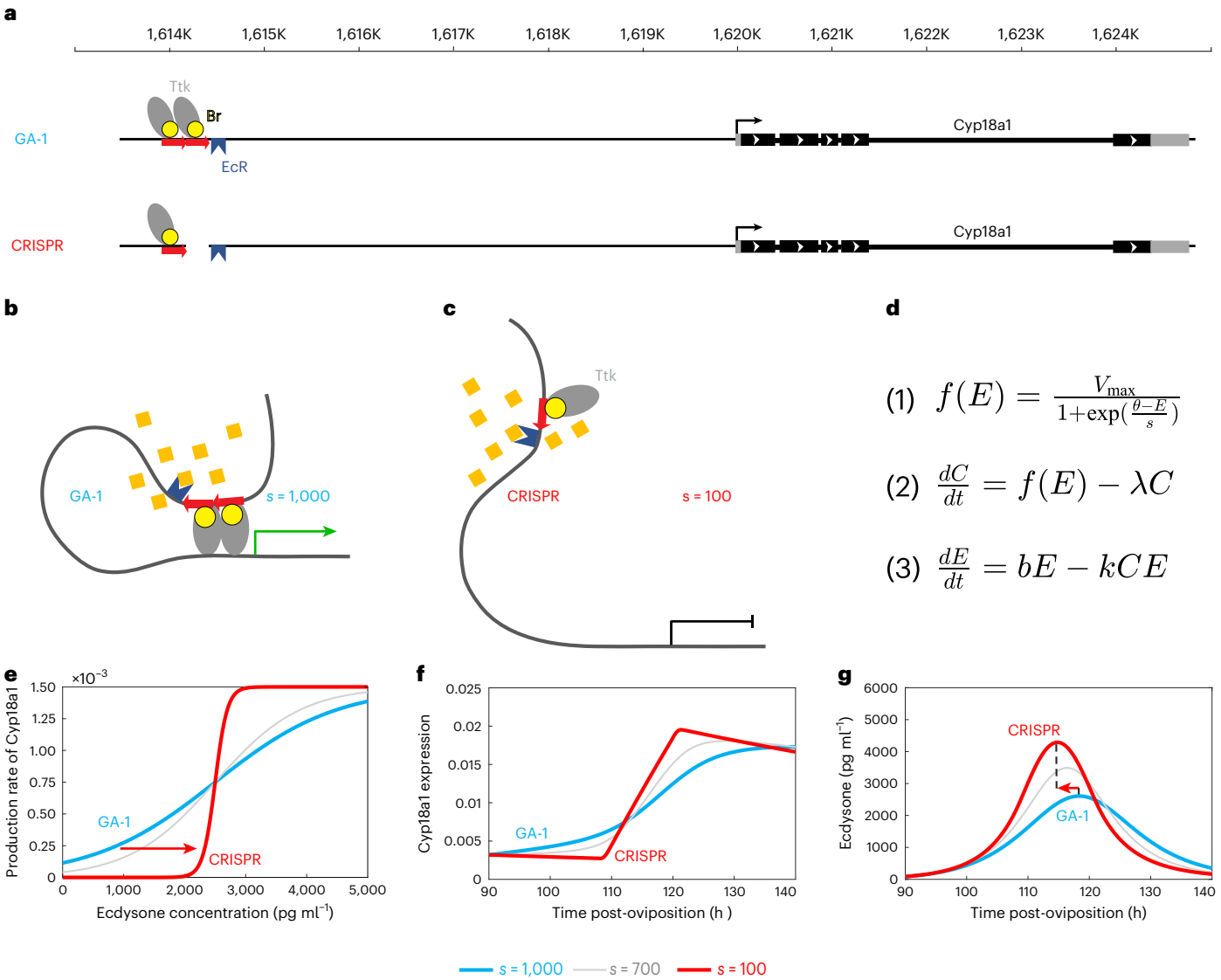

Fig. 6 | Altered regulation of *Cyp18a1* by ecdysone leads to shifts in the ecdysone peak. a, In the whole intergenic upstream region of *Cyp18a1* (numbers are positions on chromosome 9), binding sites for Broad (Br, yellow circles) and Tramtrack (Ttk, grey ovals) were only found exactly in the repeat (red arrows), followed by an ecdysone receptor/USP binding site (EcR, dark blue). These sites are duplicated in GA-1 (light blue letters, homozygous for the S allele) and single in our CRISPR line (red letters, re-creation of F allele). **b**,**c**, We propose that the enhancer in the S allele (GA-1) with the duplicated binding sites more readily forms enhancer–promotor contact at low ecdysone levels (**b**), whereas the F allele (re-created in the CRISPR line) with the single binding sites is more refractory to ecdysone (**c**). **d**, We model *Cyp18a1* levels (*C*) as a sigmoidal function of ecdysone ($f(E)$) in which we can vary sensitivity to ecdysone (s) (equation 1) minus a degradation rate (λ) (equation 2). We assume that ecdysone levels (E) are dependent on a self-regulated positive feedback loop (b) minus its degradation by Cyp18a1 (C) (equation 3). See details in Supplementary Information. **e**, Proposed production of Cyp18a1 as function of ecdysone concentration ($f(E)$) at different sensitivities for ecdysone (s = 1,000 for GA-1, blue; s = 100 for CRISPR, red). **f**, Resulting Cyp18a1 expression over time, taking the assumptions from **e**. In CRISPR (F allele, red), *Cyp18a1* expression starts to rise later and steeper than in GA-1 (S allele, blue). **g**, Resulting ecdysone levels over time, taking the assumptions from **e**. In the CRISPR line, ecdysone peaks higher and earlier (F allele, red), as observed in the fast lines.

The chromatin architectural protein Tramtrack is generally considered a repressor[50] but can also be a strong activator[51] and is required for the ecdysone-induced upregulation of Cut[52]. Thus, our analysis of transcription factor binding sites strongly suggests that the deletion is located in an ecdysone-inducible enhancer.

To examine whether altered *Cyp18a1* induction by ecdysone could cause timing shifts in the embryonic ecdysone peak, we developed a dynamic model of these interactions (Supplementary Information). First, we assume that ecdysone levels (E) are dependent on a self-regulated positive feedback loop with strength b, dampened by the degradation of ecdysone by Cyp18a1 (C) (Fig. 6d equation 3). Further, we model the response of Cyp18a1 expression to ecdysone as a sigmoidal curve[53] which we can shape by varying a parameter (s) representing sensitivity to low ecdysone (Fig. 6d(equation 1),e). When this sensitivity to ecdysone is low (s = 100), our model predicts that Cyp18a1 expression starts later (Fig. 6f) but results in an earlier and higher ecdysone peak (Fig. 6g), as observed with the F allele. Thus, these modelled dynamics explain the quickly rising ecdysone levels as a consequence of delayed *Cyp18a1* in the presence of the F allele (Fig. 5d,e). In contrast, this sensitivity is predicted to be high (s = 1,000) in the S allele that contains additional Tramtrack and Broad binding sites and appears more prone to form enhancer–promotor interactions (Fig. 6b,c). This triggers Cyp18a1 expression and concurrent ecdysone degradation already at lower ecdysone levels (Fig. 6e,f), resulting in slower accumulation of the hormone (Fig. 6g).

Thus, these alternative sensitivities shift ecdysone peaks, and are likely to also affect larval and pupal ecdysone pulses. In the presence of the F allele, ecdysone peaks are advanced and all developmental stages are shortened (Fig. 1b,c and Extended Data Fig. 1a,b).

Discussion

Our analysis of pooled resequencing data obtained from *Tribolium castaneum* lines that have been selected for embryonic DT revealed an allele of large effect on chromosome 9. The data do not rule out the existence of other major alleles affecting DT. On the contrary, a peak in the Manhattan plot comparing the slow and the non-selected lines (Extended Data Fig. 3) suggests that there is an important allele driving slow development on chromosome 6. Moreover, in the Manhattan plot comparing the fast and non-selected lines, a further conspicuous peak is present on chromosome 3 (Fig. 2a). This suggests the presence of another fast allele of large effect. Our expression analysis and RNAi screen indicate that this allele on chromosome 3 may affect *melted* or *SLC25-35-2* (Fig. 2d,e), two adjacent genes located to the left of the centromere, which in turn is located between the two high SNP clusters (Fig. 2b). Melted is a likely candidate to influence DT. By interacting with Tsc1 and FOXO, it enhances insulin/TOR activity[54], a pivotal pathway enhancing growth rate[41,55]. It is not clear how the mitochondrial carrier protein SLC25-35-2 would affect DT. It may be possible that RNAi against *SLC25-35-2* reduces transcription of the adjacent *melted* gene, similar to the observed spreading of RNAi-induced transcriptional silencing in pericentromeric repeats of yeast[56]. Thus, it is possible that this allele on chromosome 3 and the allele on chromosome 9 studied here are the only two driving alleles causing the broad peaks on chromosomes 3 and 9 (Fig. 2a), and that all other SNPs in these areas (Fig. 2b,c) are neutral hitchhikers dragged along by linkage disequilibrium[57].

However, it is also very likely that many other alleles of smaller effect are present, especially on other chromosomes since we restricted our analysis to the two areas with highly significant SNPs on chromosomes 3 and 9 (Fig. 2a). But we may also have missed crucial alleles within these areas studied. First, the thresholds to define lead SNPs (Fig. 2b,c), or the cut-off for differential expression (Fig. 2d) may have eliminated relevant genes. For instance, a gene with a less than 2.5-fold change in expression may well have a large effect on DT. Second, differential expression in a specific embryonic tissue (for example, mesoderm or neuronal tissue) may have been masked by our approach to isolate RNA from total embryos. Lastly, although RNAi in *Tribolium* is very effective[58], we did not verify individual knockdown efficiency in the RNAi screen of this scale (Fig. 2e). Regardless of these considerations, we have successfully identified *Cyp18a1* as a main target of selection for fast embryonic development.

Cyp18a1 is a cytochrome P450. Cytochrome P450s are an extremely divergent family of genes with a plethora of functions including the detoxification of xenobiotics[59–61]. However, the Halloween genes all have highly conserved substrate recognition sites[60], and the orthology of *Tribolium Cyp18a1* with other insect *Cyp18a1* genes has been clearly established[61]. Importantly, all cytochrome P450s involved in detoxification and insecticide resistance belong to completely different branches ('clans') of the cytochrome P450 phylogeny[59,61]. Together with our experimental data, this makes it highly unlikely that *Cyp18a1* has been under selection for some other reason than its role in ecdysone dynamics.

Ecdysone dynamics have been associated with alternative life histories in previous studies. For instance, ecdysone levels differ between different morphs of the cricket *Gryllus firmus*[62], and the timing of a pupal ecdysone peak differs between seasonal morphs of the butterfly *Bicyclus anynana*[63]. Morphs of both species differ in reproductive output[62,63] and *Bicyclus* morphs also differ in DT[63]. In *Bicyclus*, precocious ecdysone injections alter DT and fecundity[64]. In both species, ecdysone dynamics responded to artificial selection on these life-history traits[65,66] including DT in *Bicyclus*[65]. Thus, evolutionary tinkering with ecdysone dynamics may be a general mechanism for altering life histories and DT. So far, a whole field of 'evolutionary endocrinology' exists[67]. Our study now reveals the molecular genetic details of a natural life-history allele affecting ecdysone dynamics.

This fast allele and the alternative S allele are both present in the original wild population that was used to set up our outbred starting population (see Extended Data Fig. 5 and first line of the Methods). Although *Tribolium* may have been associated with human food storage for a few millennia[68], maintenance of such polymorphism must have an ecological explanation. Several explanations are possible, but balancing selection appears an important force maintaining polymorphisms in a population[69]. Selection may, for instance, favour fast development and rapid adult dispersal when food sources are temporary, or allow slow development and higher fecundity when food storage is more permanent. Nevertheless, it is striking that life-history alleles with such large pleiotropic effects are present in the wild *T. castaneum* population. These alleles mediated the observed experimental evolvability of DT, a trait that is thought to be highly optimized and canalized[5–7]. Classically, quantitative traits were thought to be determined by many alleles of small effect[70,71] and natural selection is expected to purge large-effect mutations in critical regions determining complex traits[72]. Our study, however, demonstrates the existence of large-effect life-history alleles in a natural population. We suggest that such alleles are likely to be crucial when insect developmental time has to adapt rapidly to current global warming.

Methods

Artificial selection

Around 40 beetles were obtained from a bakery in the Netherlands. This population was expanded until 125 male and 125 female pupae could be collected for 250 individual virgin crosses with an individual virgin beetle from the San Bernardino lab strain. Offspring from these crosses were mixed and allowed to mate randomly for another 7 generations. From this outbred strain, we obtained a 2 h egg lay. These eggs were placed on a small sieve above a funnel. Eggs did not fall through this sieve, but freshly hatched larvae fell or crawled through the sieve immediately and were collected with a device ('the selection machine') that rotates a fresh tube under the funnel every 2 h (see https://www.youtube.com/watch?v=T-hXTMS8gb0). In every tube, individuals were counted, their developmental time was registered and selection differentials were calculated. We selected the fastest 50% of individuals for the fast line (F) and the slowest half for the slow line (S). However, we never included larvae from the middle tube that contained larvae with exact median embryonic DT. This procedure was repeated for the B lines with another 2 h egg lay from the outbred strain. Independent 2-h egg lays were collected for each of the non-selected lines and also placed on the selection machine to measure embryonic DT. Using this semi-automated set-up, we continued to select the earliest-hatching half of the larvae for the fast line (F) and the latest-hatching half for the slow line (S) for 21 generations (or 17 for the slow lines). Eggs for the next generation were collected as soon as all beetles in a box were mature. If necessary, 2-h egg lays and selection rounds were repeated to keep adult populations of the next generation constant at $n = 500$. At these densities, effective population size is estimated to be ~400 (ref. 73). All populations were kept on wheat flour supplemented with 5% (w/w) dry yeast powder. Stock keeping and artificial selection were performed at 25 °C at 65% relative humidity. When displaying DT of the slow lines (Fig. 1a), we zeroed against the measurement in the non-selected lines that was closest in time (and not of the same generation) to minimize distortion by slightly different environmental conditions.

Life-history traits

Forty-eight freshly hatched larvae (maximum 4 h old) of each selection line were individually placed in a well of a 24-well plate with a little 5% yeast-supplemented wheat flour and kept at 25 °C. Moults were monitored daily. Freshly pupariated pupae and newly emerged

adults were weighed on a Mettler Toledo XS105 balance. To measure early fecundity, 50 males and 50 females were put in a Petri dish with 5% yeast-supplemented wheat flour in duplicate for each selection line. The eggs that these beetles laid in 4 h on fine, pure wheat flour were sieved out with a 300 µm sieve and counted. This process was repeated three times for each duplicate. To measure longevity, 20 freshly eclosed females and 10 freshly eclosed males of each selection line were put into a Petri dish with 5% yeast-supplemented wheat flour in triplicate. Mortality was logged weekly. Fecundity and longevity were measured at 30 °C and 50% relative humidity.

For each phenotype, the effect of selection treatment was tested using a mixed-effects analysis of variance (ANOVA) in R (v.3.6.1), where the line identities (A/B) were fitted as random effects. First, we fitted three models, with treatment (fast, ns, slow) and sex (Mcomplete) and two models without treatment (Msex) using lmer (lme4 package). Then, we contrasted these two models using the anova function (Mcomplete, Msex) to test for the effect of sex. Only when sex had a significant effect was the model kept in further tests and shown separately in graphs (see Extended Data Fig. 1). Similarly as above, we then tested for the effect of treatment by fitting the complete model (Mcomplete) and without treatment (Mtreatment) and contrasted these using the anova function (Mcomplete, Mtreatment). The significance of the test was assessed using the χ^2 statistic and considered significant if the P value was below 0.05. For each trait, the effect of treatment (fast, ns, slow) was generally tested and as a post-hoc test, each pairwise difference between treatments (fast vs slow, slow vs ns and ns vs fast) was tested in a similar way. For lifespan, a Cox mixed-effects model was fitted, using the coxme package[74] in R, where the effect of selection regime was used as a fixed factor, and replicate line and replicate tube were used as nested random effects. A model without selection regime was used as null hypothesis and significance was tested using the anova (full model, H0, test='Chi') function.

Embryo fixation and DAPI staining

Eggs were dechorionated in commercial bleach (5% NaClO), fixed for 20 min in a 1:1 mixture of heptane and 3.7% formaldehyde in PBS, and devitellinized using a methanol shock for subsequent 15 min DAPI staining and washes in PBST. Embryos were photographed under a Zeiss Axioplan 2 microscope.

Pooled resequencing and SNP analysis

Approximately 100 eggs of each selection line were dechorionated in commercial bleach (5% NaClO) and washed well with tap water. DNA was extracted using a standard phenol-chloroform extraction (phenol :chloroform:isoamyl-alcohol 25:24:1). The pooled DNA was sequenced on an Illumina Hiseq4000 machine with a paired-end 150-bp layout. Reads have been deposited as NCBI BioProject PRJNA942224.

The raw reads were trimmed using TRIMMOMATIC (v.0.27, LEADING:3, TRAILING:3, SLIDINGWINDOW:4:15, MINLENGTH:70)[75]. The trimmed reads were aligned on the Tcas 5.2 (GCF_000002335.3) genome using bwa mem (v.0-7-15, default parameters, https://arxiv.org/abs/1303.3997). After mapping, reads were filtered for quality (20) and sorted using samtools (v.0.1.19)[76]. We then removed duplicates using picard tools (v.2.8.2, http://picard.sourceforge.net) and performed realignment around indels with GATK (v.3.7-0)[77]. The resulting BAM files were combined in mpileup format (samtools, mpileup, default parameters, v.0.1.19)[76], after which SNPs and indels were separately called using varscan (v.2.3.9, using mpileup2snps and mpileup2indel resp., –output-vcf 1, –min-var-freq 0.05)[78] for which we only kept those variants that differed between the samples. The resulting raw vcf files were then annotated with snpEff (v.4.3)[79] using the Tcas 5.2 GCF_000002335.3 annotation file (GFF)[80] as input.

The resulting vcf files were further filtered using the R (v.3.6.1) package vcfR (v.1.8.0)[81]. For the contrast between the fast and non-selected treatments, as well as the slow and non-selected treatments, a similar approach was used. Only biallelic SNPs were analysed that had a minimum coverage between the 0.05 and 0.98 quantiles (using the quantile() function) of total depth for all samples. Furthermore, SNPs were removed if they lay near indels (<10 bp) and if they were not present on the major chromosome scaffolds. A GLM was fitted with binomial error structure testing for treatments against non-selected lines, which was previously shown to be a powerful test for evolve-and resequence experiments[38]. To create an H_0 permutated P value distribution, the two other possible sample configurations were used and a GLM was also run. For instance, for fast against non-selected, we tested FastA and FastB against NSA and NSB as the observed GLM. Then FastA and NSA were tested against FastB and NSB as the first permutation and FastA and NSB were tested against FastB and NSA as a second permutation. These two permutated distributions were then used to calculate the permutated P value distribution (empPvals(observed,c(H0_1,H0_2), pool=TRUE)), and the resulting permutated P values were transformed into q values using the qvalue function (qvalue package). Loci were considered significant when this q value was below 0.01. Lead SNPs had an allele frequency change >0.6 and a $-\log_e(P) > 58.5$ for chromosome 3, or >60.5 for chromosome 9, and did not have a higher SNP within ~10 kb distance. Code is available in Zenodo at https://doi.org/10.5281/zenodo.839504883.

RNA isolation, cDNA synthesis and qPCR

RNA was extracted from 200–300 eggs from each selection line at the desired timepoint after a 2-h egg lay using Trizol (Invitrogen) extraction, followed by DNA digestion and purification over an RNeasy column (Qiagen). Total RNA (1 µg) was used for cDNA synthesis (Promega reverse transcription system). Diluted cDNA (2 µl, 1:10) was used for RT–qPCR with the Universal SYBR Green Supermix (Biorad) on a CFX96 thermocycler (Biorad). Thermal conditions were 95 °C for 30 s, followed by 40 cycles of 95 °C for 15 s, 60 °C for 30 s and 72 °C for 30 s. Primer sequences can be found in Supplementary Table 4. RPL13a was used as reference gene[82]. Relative expression was calculated with reference to the average of the non-selected lines (Fig. 2) or a defined timepoint (Fig. 3) using the $2^{-\Delta\Delta C_t}$ method[83], or presented as a fraction of RPL13a expression (Fig. 4). All experiments were performed with two biological replicates measured in two technical replicates. Unpaired t-tests were used to determine significant differences between the fold change in the fast lines with that in the non-selected lines.

RNAi

Gene fragments (see primers and product sizes in Supplementary Table 4) were cloned into the TOPO II vector (Invitrogen) and inserts were confirmed by Sanger sequencing. The plasmids were linearized with an appropriate restriction enzyme to generate DNA templates for in vitro transcription with SP6 and T7 polymerases, and the resulting double-stranded RNA (dsRNA) was purified using the Ambion MEGAscript RNAi kit. Parental RNAi in female adults of the GA-1 laboratory strain was performed as previously described[84]. Two-hour egg lays were placed on the selection machine (see 'Artificial selection') to measure developmental time next to a control RNAi with dsRNA from a 500-bp bacterial vector sequence without target in the *Tribolium* genome[85]. Measurements were performed in triplicate and the significance of the difference from control developmental time was determined using a Student's t-test.

Ecdysone detection

At the desired timepoint after a 2-h egg lay, ~50 eggs were dechorionated in 0.5% bleach for 2 min, homogenized in 300 µl of methanol and centrifuged for 10 min at 12,000 × g. The supernatant was collected into a new 1.5 ml tube, dried completely in a vacuum centrifuge and the precipitate was redissolved in 120 µl EIA buffer provided by a competitive enzyme immune assay (EIA) kit for 20-hydroxyecdysone (Bertin Pharma). After a 2-h incubation at room temperature, the samples were

diluted 4 times in EIA buffer and applied to the detection plate following manufacturer protocol. For measuring ecdysone levels after RNAi (Fig. 3d), fewer living eggs were used and dilution was adjusted. The plate was developed with 200 µl of Ellman's reagent and incubated with an orbital shaker in the dark at r.t. After 90 min, the plate was measured at a wavelength of 410 nm on a Tecan Spark microplate reader. The concentrations were determined by a four-parameter logistic fitting.

In situ hybridization

A 1,124-bp fragment of *Cyp18a1* and an 837-bp fragment of Spo were cloned into TOPO II vector (Invitrogen) and sequenced (see primers in Supplementary Table 4). Templates were generated using M13 primers. DIG-labelled antisense probes were synthesized using SP6 polymerase for *Cyp18a1* and T7 polymerase (Ambion) with Roche RNA labelling mix. Sense probes were synthesized as control. In situ hybridizations on whole-mount fixed eggs (see 'Embryo fixation and DAPI staining') were essentially performed as described in ref. 86 but without the ProteinaseK step.

Reassembly of Illumina reads around *Cyp18a1* lead SNP

Using IGV (v.2.8.0)[87], visual inspection of the Illumina reads mapping around the *Cyp18a1* lead SNP P5/A12 (reference genome position 1,613,665) detected a conspicuous drop in coverage on a repeated sequence, suggesting a deletion. To reassemble this region, we identified three *k*mers (ATATTTTTGGTTACTGTTTTTGATAGCAGATATTCTC, GATTGTTTTTTTGCTTATTTTAAAATCACTCT and AATACCGACAGTAAAAGTTTCACTTAATGACTT) that lay before, within and after the duplication, respectively, and searched for reads containing these sequences using BBduk (v.38.91, https://sourceforge.net/projects/bbmap/) with default settings. Both the forward and reverse reads that matched were fed into SPAdes (v.3.13.1)[88] for both the control and fast lines, resulting in scaffolds that were then compared to the reference genome[80].

PCR genotyping

DNA from individual beetles was extracted using phenol-chloroform extraction (phenol:chloroform:isoamyl-alcohol 25:24:1) after 1.5 µg µl^{-1} proteinaseK incubation overnight at 55 °C. PCRs with Bio SeqAMP polymerase (Takara) using the primers 5′-AAGGGGCCCTCTCAAACATC-3′ and 5′-CAGGCACCTCTGCGTTATCC-3′ generated a 942-bp band for homozygotes containing both repeats, a 720-bp band for homozygotes for the deletion and both bands plus a hybrid band running slower because of the formed loop for the heterozygotes.

Population genetic modelling

Using the genotyping data from generations 0, 3, 7, 10 and 21, we fitted a model with and without fitness (w) differences for the three genotypes using R (v.3.6.1). For each generation, the initial allele frequency for F was fitted. For each of the parameter settings, the model was calculated forward and the multinomial probability of finding the actual genotype counts was calculated and denoted as the likelihood of the model. The two models, with or without selection, were then tested for significant difference using the likelihood ratio test, which was tested against the χ^2 distribution using

$$\chi 2 = -2(L_{wFF==wFS==wSS} - L_{wFF!=wFS!=wSS})$$

where L is the log likelihood. The models were fitted starting from the estimated initial frequency for F, using the count data at generation 0 and equal fitness values for the genotypes FF, FS and SS. Then the likelihood of the model was calculated and the parameters updated using a change randomly drawn from a normal distribution (mean 0, s.d. 0.01). The new parameters for allele frequency were limited such that they were not smaller than 0 or larger than 1. For fitness, the changes were not allowed to become lower than 0. At each iteration, the maximum fitness was set to 1. When the likelihood of the model was higher than the previous best fit, the parameters were updated using the new best-fit parameters. Code is available in Zenodo at https://doi.org/10.5281/zenodo.8395048 ref. 89.

CRISPR/Cas9

The oligonucleotides 5′-AGTGAAATATAGGGTGTTCCATT-3′ and 5′-AAACAATGGAACACCCTATATTT-3′ were ligated into the BsaI-digested p(U6a-BsaI-gRNA) vector[90] (Addgene) for in vivo expression of the desired gRNA (gRNA sequence green in Supplementary Data 3). This construct and the TrueCut Cas9 Protein v2 (Invitrogen) were co-injected each at a concentration of 500 ng µl^{-1} into 2-hour-old embryos of the Georgia laboratory strain according to ref. 91. Single crosses of virgin G0 animals were set up and their G1 offspring was collected. A PCR (as described above for genotyping) on the mosaic G0 parents was performed to get an impression of excision efficiency. Offspring from G0 parents that still showed the repeat containing the 942-bp band (the S allele) was rejected. Among the remaining G1 offspring, single virgin crosses were set-up and their G2 offspring was collected. The non-mosaic G1 parents were genotyped by Sanger sequencing until all four parental alleles were recovered to choose the G2 offspring to set up a stock. The alleles present in the stock exactly reproduced the F allele with a maximum indel of 9 bp around the protospacer adjacent motif (PAM) (Supplementary Data 3).

Live imaging

Two hundred females of the nGFP line[47] were selected at the pupal stage and 100 of these females were crossed with 100 males of GA-1, and the other 100 females were crossed with 100 males of the CRISPR line (see above). These two groups of 200 parents were allowed to lay eggs for 20 min, and 10–15 of their eggs were imaged under a NikonAX confocal microscope taking full scans every 26 min.

Binding site analysis

Binding matrices for Br(var.4), Ttk and EcR::usp were downloaded from JASPAR[92] and used to search motifs in the whole intergenic region upstream of *Cyp18a1* (chromosome 9: NC_007424.3(1611573.1619999)) with FIMO[48].

Mathematical modelling of Cyp18a1/ecdysone regulation

See Supplementary Information.

Reporting summary

Further information on research design is available in the Nature Portfolio Reporting Summary linked to this article.

Data availability

Sequencing reads have been deposited in NCBIs Sequencing Read Archive as BioProject PRJNA942224. All other data are provided as supplementary data files. Source data are provided with this paper.

Code availability

All custom code is available in Zenodo at https://doi.org/10.5281/zenodo.8395048 ref. 89. All other code used is referenced.

References

1. Dobreva, M. P., Camacho, J. & Abzhanov, A. Time to synchronize our clocks: connecting developmental mechanisms and evolutionary consequences of heterochrony. *J. Exp. Zool. B* **338**, 87–106 (2022).
2. Gould, S. J. *Ontogeny and Phylogeny* (Harvard Univ. Press, 1977).
3. Roff, D. A. *The Evolution of Life Histories: Theory and Analysis* (Chapman & Hall, 1992).
4. Stearns, S. C. *The Evolution of Life Histories* (Oxford Univ. Press, 1992).

5. Stearns, S. C. Life history evolution: successes, limitations, and prospects. *Naturwissenschaften* **87**, 476–486 (2000).
6. Stearns, S. C., Kaiser, M. & Kawecki, T. J. The differential genetic and environmental canalization of fitness components in *Drosophila melanogaster*. *J. Evol. Biol.* **8**, 539–557 (1995).
7. Stearns, S. C. & Kawecki, T. J. Fitness sensitivity and the canalization of life-history traits. *Evolution* **48**, 1438–1450 (1994).
8. Kharouba, H. M. et al. Global shifts in the phenological synchrony of species interactions over recent decades. *Proc Natl Acad. Sci. USA* **115**, 5211–5216 (2018).
9. Samplonius, J. M. et al. Strengthening the evidence base for temperature-mediated phenological asynchrony and its impacts. *Nat. Ecol. Evol.* **5**, 155–164 (2021).
10. Thackeray, S. J. et al. Phenological sensitivity to climate across taxa and trophic levels. *Nature* **535**, 241–245 (2016).
11. Singer, M. C. & Parmesan, C. Phenological asynchrony between herbivorous insects and their hosts: signal of climate change or pre-existing adaptive strategy? *Phil. Trans. R. Soc. B* **365**, 3161–3176 (2010).
12. Visser, M. E. & Gienapp, P. Evolutionary and demographic consequences of phenological mismatches. *Nat. Ecol. Evol.* **3**, 879–885 (2019).
13. van Asch, M., Salis, L., Holleman, L. J. M., van Lith, B. & Visser, M. E. Evolutionary response of the egg hatching date of a herbivorous insect under climate change. *Nat. Clim. Change* **3**, 244–248 (2013).
14. Franks, S. J. & Hoffmann, A. A. Genetics of climate change adaptation. *Annu. Rev. Genet.* **46**, 185–208 (2012).
15. Renner, S. S. & Zohner, C. M. Climate change and phenological mismatch in trophic interactions among plants, insects, and vertebrates. *Annu. Rev. Ecol. Evol. Syst.* **49**, 165–182 (2018).
16. Mensch, J. et al. Identifying candidate genes affecting developmental time in *Drosophila melanogaster*: pervasive pleiotropy and gene-by-environment interaction. *BMC Dev. Biol.* **8**, 78 (2008).
17. Flatt, T. Life-history evolution and the genetics of fitness components in *Drosophila melanogaster*. *Genetics* **214**, 3–48 (2020).
18. Horvath, B., Betancourt, A. J. & Kalinka, A. T. A novel method for quantifying the rate of embryogenesis uncovers considerable genetic variation for the duration of embryonic development in *Drosophila melanogaster*. *BMC Evol. Biol.* **16**, 200 (2016).
19. Chippindale, A. K., Alipaz, J. A., Chen, H. W. & Rose, M. R. Experimental evolution of accelerated development in *Drosophila*.1. Developmental speed and larval survival. *Evolution* **51**, 1536–1551 (1997).
20. Nunney, L. The response to selection for fast larval development in *Drosophila melanogaster* and its effect on adult weight: an example of a fitness trade-off. *Evolution* **50**, 1193–1204 (1996).
21. Prasad, N. G. et al. Evolution of reduced pre-adult viability and larval growth rate in laboratory populations of *Drosophila melanogaster* selected for shorter development time. *Genet. Res.* **76**, 249–259 (2000).
22. Sharma, K., Mishra, N. & Shakarad, M. N. Evolution of reduced minimum critical size as a response to selection for rapid pre-adult development in *Drosophila melanogaster*. *R. Soc. Open Sci.* **7**, 191910 (2020).
23. Zwaan, B., Bijlsma, R. & Hoekstra, R. F. Artificial selection for developmental time in *Drosophila melanogaster* in relation to the evolution of aging: direct and correlated responses. *Evolution* **49**, 635–648 (1995).
24. Fischer, K., Zwaan, B. J. & Brakefield, P. M. Realized correlated responses to artificial selection on pre-adult life-history traits in a butterfly. *Heredity* **98**, 157–164 (2007).
25. Seslija, D. & Tucic, N. Selection for developmental time in bean weevil (*Acanthoscelides obtectus*): correlated responses for other life history traits and genetic architecture of line differentiation. *Entomol. Exp. Appl.* **106**, 19–35 (2003).
26. Soliman, M. H. Directional and stabilizing selection for developmental time and correlated response in reproductive fitness in *Tribolium castaneum*. *Theor. Appl. Genet.* **63**, 111–116 (1982).
27. Nascimento, J. C. D., Cruz, I. B. M. D., Monjeló, L. A. & Oliveira, A. K. D. Genetic components affecting embryonic developmental time of *Drosophila melanogaster*. *Genet. Mol. Biol.* **25**, 157–160 (2002).
28. Neyfakh, A. A. & Hartl, D. L. Genetic control of the rate of embryonic development: selection for faster development at elevated temperatures. *Evolution* **47**, 1625–1631 (1993).
29. Marinkovic, D. & Ayala, F. J. Selection for different rates of embryonic development in *Drosophila melanogaster* and *Drosophila simulans*. *Genetika* **18**, 205–219 (1986).
30. Long, A., Liti, G., Luptak, A. & Tenaillon, O. Elucidating the molecular architecture of adaptation via evolve and resequence experiments. *Nat. Rev. Genet.* **16**, 567–582 (2015).
31. Klingler, M. & Bucher, G. The red flour beetle *T. castaneum*: elaborate genetic toolkit and unbiased large scale RNAi screening to study insect biology and evolution. *Evodevo* **13**, 14 (2022).
32. Richards, S. et al. The genome of the model beetle and pest *Tribolium castaneum*. *Nature* **452**, 949–955 (2008).
33. Flatt, T. & Heyland, A. *Mechanisms of Life History Evolution: The Genetics and Physiology of Life History Traits and Trade-offs* (Oxford Univ. Press, 2011).
34. Roff, D. A. Trade-offs between growth and reproduction: an analysis of the quantitative genetic evidence. *J. Evol. Biol.* **13**, 434–445 (2000).
35. Lee, Y. et al. Inverse correlation between longevity and developmental rate among wild *C. elegans* strains. *Aging* **8**, 986–999 (2016).
36. Panfilio, K. A. Extraembryonic development in insects and the acrobatics of blastokinesis. *Dev. Biol.* **313**, 471–491 (2008).
37. Schlotterer, C., Tobler, R., Kofler, R. & Nolte, V. Sequencing pools of individuals – mining genome-wide polymorphism data without big funding. *Nat. Rev. Genet.* **15**, 749–763 (2014).
38. Hoedjes, K. M. et al. Distinct genomic signals of lifespan and life history evolution in response to postponed reproduction and larval diet in *Drosophila*. *Evol. Lett.* **3**, 598–609 (2019).
39. Guittard, E. et al. CYP18A1, a key enzyme of *Drosophila* steroid hormone inactivation, is essential for metamorphosis. *Dev. Biol.* **349**, 35–45 (2011).
40. Rewitz, K. F., Yamanaka, N. & O'Connor, M. B. Steroid hormone inactivation is required during the juvenile–adult transition in *Drosophila*. *Dev. Cell* **19**, 895–902 (2010).
41. Nijhout, H. F. et al. The developmental control of size in insects. *Wiley Interdiscip. Rev. Dev. Biol.* **3**, 113–134 (2014).
42. Niwa, Y. S. & Niwa, R. Transcriptional regulation of insect steroid hormone biosynthesis and its role in controlling timing of molting and metamorphosis. *Dev. Growth Differ.* **58**, 94–105 (2016).
43. Kozlova, T. & Thummel, C. S. Essential roles for ecdysone signaling during *Drosophila* mid-embryonic development. *Science* **301**, 1911–1914 (2003).
44. Maroy, P., Kaufmann, G. & Dubendorfer, A. Embryonic ecdysteroids of *Drosophila melanogaster*. *J. Insect Physiol.* **34**, 633–637 (1988).
45. Yoo, B. et al. 20-hydroxyecdysone (20E) signaling regulates amnioserosa morphogenesis during *Drosophila* dorsal closure: EcR modulates gene expression in a complex with the AP-1 subunit, Jun. *Biol. Open* **10**, bio058605 (2021).
46. Kidokoro, K., Wata, K., Fujiwara, Y. & Takeda, M. Effects of juvenile hormone analogs and 20-hydroxyecdysone on diapause termination in eggs of *Locusta migratoria* and *Oxya yezoensis*. *J. Insect Physiol.* **52**, 473–479 (2006).

47. Sarrazin, A. F., Peel, A. D. & Averof, M. A segmentation clock with two-segment periodicity in insects. *Science* **336**, 338–341 (2012).
48. Grant, C. E., Bailey, T. L. & Noble, W. S. FIMO: scanning for occurrences of a given motif. *Bioinformatics* **27**, 1017–1018 (2011).
49. Karim, F. D., Guild, G. M. & Thummel, C. S. The *Drosophila* Broad-Complex plays a key role in controlling ecdysone-regulated gene expression at the onset of metamorphosis. *Development* **118**, 977–988 (1993).
50. Pagans, S., Ortiz-Lombardia, M., Espinas, M. L., Bernues, J. & Azorin, F. The *Drosophila* transcription factor tramtrack (TTK) interacts with Trithorax-like (GAGA) and represses GAGA-mediated activation. *Nucleic Acids Res.* **30**, 4406–4413 (2002).
51. Yu, Y., Yussa, M., Song, J. B., Hirsch, J. & Pick, L. A double interaction screen identifies positive and negative ftz gene regulators and Ftz-interacting proteins. *Mech. Dev.* **83**, 95–105 (1999).
52. Sun, J., Smith, L., Armento, A. & Deng, W. M. Regulation of the endocycle/gene amplification switch by Notch and ecdysone signaling. *J. Cell Biol.* **182**, 885–896 (2008).
53. Zuin, J. et al. Nonlinear control of transcription through enhancer-promoter interactions. *Nature* **604**, 571–577 (2022).
54. Teleman, A. A., Chen, Y. W. & Cohen, S. M. *Drosophila* melted modulates FOXO and TOR activity. *Dev. Cell* **9**, 271–281 (2005).
55. Baker, K. D. & Thummel, C. S. Diabetic larvae and obese flies–emerging studies of metabolism in *Drosophila*. *Cell Metab.* **6**, 257–266 (2007).
56. Noma, K. et al. RITS acts in *cis* to promote RNA interference-mediated transcriptional and post-transcriptional silencing. *Nat. Genet.* **36**, 1174–1180 (2004).
57. Franssen, S. U., Nolte, V., Tobler, R. & Schlotterer, C. Patterns of linkage disequilibrium and long range hitchhiking in evolving experimental *Drosophila melanogaster* populations. *Mol. Biol. Evol.* **32**, 495–509 (2015).
58. Horn, T., Narov, K. D. & Panfilio, K. A. Persistent parental RNAi in the beetle *Tribolium castaneum* involves maternal transmission of long double-stranded RNA (Advanced Genetics 3/03). *Adv. Genet.* **3**, 2270031 (2022).
59. Dermauw, W., Van Leeuwen, T. & Feyereisen, R. Diversity and evolution of the P450 family in arthropods. *Insect Biochem. Mol. Biol.* **127**, 103490 (2020).
60. Rewitz, K. F., O'Connor, M. B. & Gilbert, L. I. Molecular evolution of the insect Halloween family of cytochrome P450s: phylogeny, gene organization and functional conservation. *Insect Biochem. Mol. Biol.* **37**, 741–753 (2007).
61. Zhu, F., Moural, T. W., Shah, K. & Palli, S. R. Integrated analysis of cytochrome P450 gene superfamily in the red flour beetle, *Tribolium castaneum*. *BMC Genomics* **14**, 174 (2013).
62. Zera, A. J., Zhao, Z. & Kaliseck, K. Hormones in the field: evolutionary endocrinology of juvenile hormone and ecdysteroids in field populations of the wing-dimorphic cricket *Gryllus firmus*. *Physiol. Biochem. Zool.* **80**, 592–606 (2007).
63. Oostra, V. et al. Translating environmental gradients into discontinuous reaction norms via hormone signalling in a polyphenic butterfly. *Proc. Biol. Sci.* **278**, 789–797 (2011).
64. Oostra, V. et al. Ecdysteroid hormones link the juvenile environment to alternative adult life histories in a seasonal insect. *Am. Nat.* **184**, E79–E92 (2014).
65. Zijlstra, W. G., Steigenga, M. J., Koch, P. B., Zwaan, B. J. & Brakefield, P. M. Butterfly selected lines explore the hormonal basis of interactions between life histories and morphology. *Am. Nat.* **163**, E76–E87 (2004).
66. Zera, A. J. & Bottsford, J. The endocrine-genetic basis of life-history variation: the relationship between the ecdysteroid titer and morph-specific reproduction in the wing-polymorphic cricket *Gryllus firmus*. *Evolution* **55**, 538–549 (2001).
67. Zera, A. J., Harshman, L. G. & Williams, T. D. Evolutionary endocrinology: the developing synthesis between endocrinology and evolutionary genetics. *Annu. Rev. Ecol. Evol. Syst.* **38**, 793–817 (2007).
68. Pointer, M. D., Gage, M. J. G. & Spurgin, L. G. *Tribolium* beetles as a model system in evolution and ecology. *Heredity* **126**, 869–883 (2021).
69. Charlesworth, B. Causes of natural variation in fitness: evidence from studies of *Drosophila* populations. *Proc. Natl Acad. Sci. USA* **112**, 1662–1669 (2015).
70. Charlesworth, B. & Edwards, A. W. A century of variance. *Significance* **15**, 20–25 (2018).
71. Dittmar, E. L., Oakley, C. G., Conner, J. K., Gould, B. A. & Schemske, D. W. Factors influencing the effect size distribution of adaptive substitutions. *Proc. Biol. Sci.* **283**, 20153065 (2016).
72. O'Connor, L. J. et al. Extreme polygenicity of complex traits is explained by negative selection. *Am. J. Hum. Genet.* **105**, 456–476 (2019).
73. Pray, L. A., Goodnight, C. J., Stevens, L., Schwartz, J. M. & Yan, G. Y. The effect of population size on effective population size: an empirical study in the red flour beetle *Tribolium castaneum*. *Genet. Res.* **68**, 151–155 (1996).
74. Therneau, T. M., Grambsch, P. M. & Pankratz, V. S. Penalized survival models and frailty. *J. Comput. Graph. Stat.* **12**, 156–175 (2003).
75. Bolger, A. M., Lohse, M. & Usadel, B. Trimmomatic: a flexible trimmer for Illumina sequence data. *Bioinformatics* **30**, 2114–2120 (2014).
76. Li, H. et al. The Sequence Alignment/Map format and SAMtools. *Bioinformatics* **25**, 2078–2079 (2009).
77. McKenna, A. et al. The Genome Analysis Toolkit: a MapReduce framework for analyzing next-generation DNA sequencing data. *Genome Res.* **20**, 1297–1303 (2010).
78. Koboldt, D. C. et al. VarScan: variant detection in massively parallel sequencing of individual and pooled samples. *Bioinformatics* **25**, 2283–2285 (2009).
79. Cingolani, P. et al. A program for annotating and predicting the effects of single nucleotide polymorphisms, SnpEff: SNPs in the genome of *Drosophila melanogaster* strain w(1118); iso-2; iso-3. *Fly* **6**, 80–92 (2012).
80. Herndon, N. et al. Enhanced genome assembly and a new official gene set for *Tribolium castaneum*. *BMC Genomics* **21**, 47 (2020).
81. Knaus, B. J. & Grunwald, N. J. VCFR: a package to manipulate and visualize variant call format data in R. *Mol. Ecol. Resour.* **17**, 44–53 (2017).
82. Lord, J. C., Hartzer, K., Toutges, M. & Oppert, B. Evaluation of quantitative PCR reference genes for gene expression studies in *Tribolium castaneum* after fungal challenge. *J. Microbiol. Methods* **80**, 219–221 (2010).
83. Livak, K. J. & Schmittgen, T. D. Analysis of relative gene expression data using real-time quantitative PCR and the 2(-Delta Delta C(T)) Method. *Methods* **25**, 402–408 (2001).
84. van der Zee, M., Stockhammer, O., von Levetzow, C., Nunes da Fonseca, R. & Roth, S. Sog/Chordin is required for ventral-to-dorsal Dpp/BMP transport and head formation in a short germ insect. *Proc. Natl Acad. Sci. USA* **103**, 16307–16312 (2006).
85. Jacobs, C. G., Rezende, G. L., Lamers, G. E. & van der Zee, M. The extraembryonic serosa protects the insect egg against desiccation. *Proc. R. Soc. B* **280**, 20131082 (2013).
86. Tautz, D. & Pfeifle, C. A non-radioactive in situ hybridization method for the localization of specific RNAs in *Drosophila* embryos reveals translational control of the segmentation gene hunchback. *Chromosoma* **98**, 81–85 (1989).

87. Robinson, J. T. et al. Integrative genomics viewer. *Nat. Biotechnol.* **29**, 24–26 (2011).
88. Bankevich, A. et al. SPAdes: a new genome assembly algorithm and its applications to single-cell sequencing. *J. Comput. Biol.* **19**, 455–477 (2012).
89. Cheng, S. et al. Rcode for ChengNEE2023. *Zenodo* https://doi.org/10.5281/zenodo.8395048 (2023).
90. Gilles, A. F., Schinko, J. B. & Averof, M. Efficient CRISPR-mediated gene targeting and transgene replacement in the beetle *Tribolium castaneum*. *Development* **142**, 2832–2839 (2015).
91. Berghammer, A. J., Weber, M., Trauner, J. & Klingler, M. Red flour beetle (*Tribolium*) germline transformation and insertional mutagenesis. *Cold Spring Harb. Protoc.* **2009**, pdb prot5259 (2009).
92. Castro-Mondragon, J. A. et al. JASPAR 2022: the 9th release of the open-access database of transcription factor binding profiles. *Nucleic Acids Res.* **50**, D165–D173 (2022).
93. Handel, K., Grunfelder, C. G., Roth, S. & Sander, K. *Tribolium* embryogenesis: a SEM study of cell shapes and movements from blastoderm to serosal closure. *Dev. Genes Evol.* **210**, 167–179 (2000).
94. Hilbrant, M., Horn, T., Koelzer, S. & Panfilio, K. A. The beetle amnion and serosa functionally interact as apposed epithelia. *Elife* **5**, e13834 (2016).

Acknowledgements

We thank R. Jacobs for building the selection machine; K. Koops for taking care of the beetles; G. Lamers and J. Willemse for help with confocal live imaging; and M. Averof and B. Zwaan for experimental advice. M. Averof, P. Brakefield, M. Richardson and B. Zwaan substantially improved the manuscript. S.C. and D.C. were supported by the Chinese Scholarship Council (scholarship 201808210285 to S.C. and 201906280500 to D.C.).

Author contributions

J.v.d.H. and M.v.d.Z. share last authorship of this work. S.C. analysed and performed developmental staging, qPCR, RNAi, genotyping, ecdysone measurements, microscopy and CRISPR/Cas9 gene editing. E.A.M.P. contributed to qPCR and data analysis. J.v.d.S. contributed to RNAi and genotyping. K.M.B., F.V. and J.S.B. collected life-history data. A.H. performed in situ hybridization. C.G.C.J. performed and analysed the artificial selection process. D.C. developed and analysed the dynamic model of Cyp18a1 and ecdysone regulation. R.M.H.M. supervised this mathematical modelling. J.v.d.H. analysed and visualized the pooled resequencing data and life-history data, and developed the population genetic model. C.G.C.J. and M.v.d.Z. conceived the study. S.C., C.G.C.J., J.v.d.H. and M.v.d.Z. designed the experiments. M.v.d.Z. wrote the paper with substantial input from J.v.d.H., and feedback from S.C., C.G.C.J., E.A.M.P. and R.M.H.M.

Competing interests

The authors declare no competing interests.

Additional information

Extended data is available for this paper at https://doi.org/10.1038/s41559-023-02246-y.

Supplementary information The online version contains supplementary material available at https://doi.org/10.1038/s41559-023-02246-y.

Correspondence and requests for materials should be addressed to Maurijn van der Zee.

Peer review information *Nature Ecology & Evolution* thanks Sheng Li, Karl Gotthard, Enoch Ng'oma and the other, anonymous, reviewer(s) for their contribution to the peer review of this work. Peer reviewer reports are available.

https://doi.org/10.1038/s41559-023-02246-y

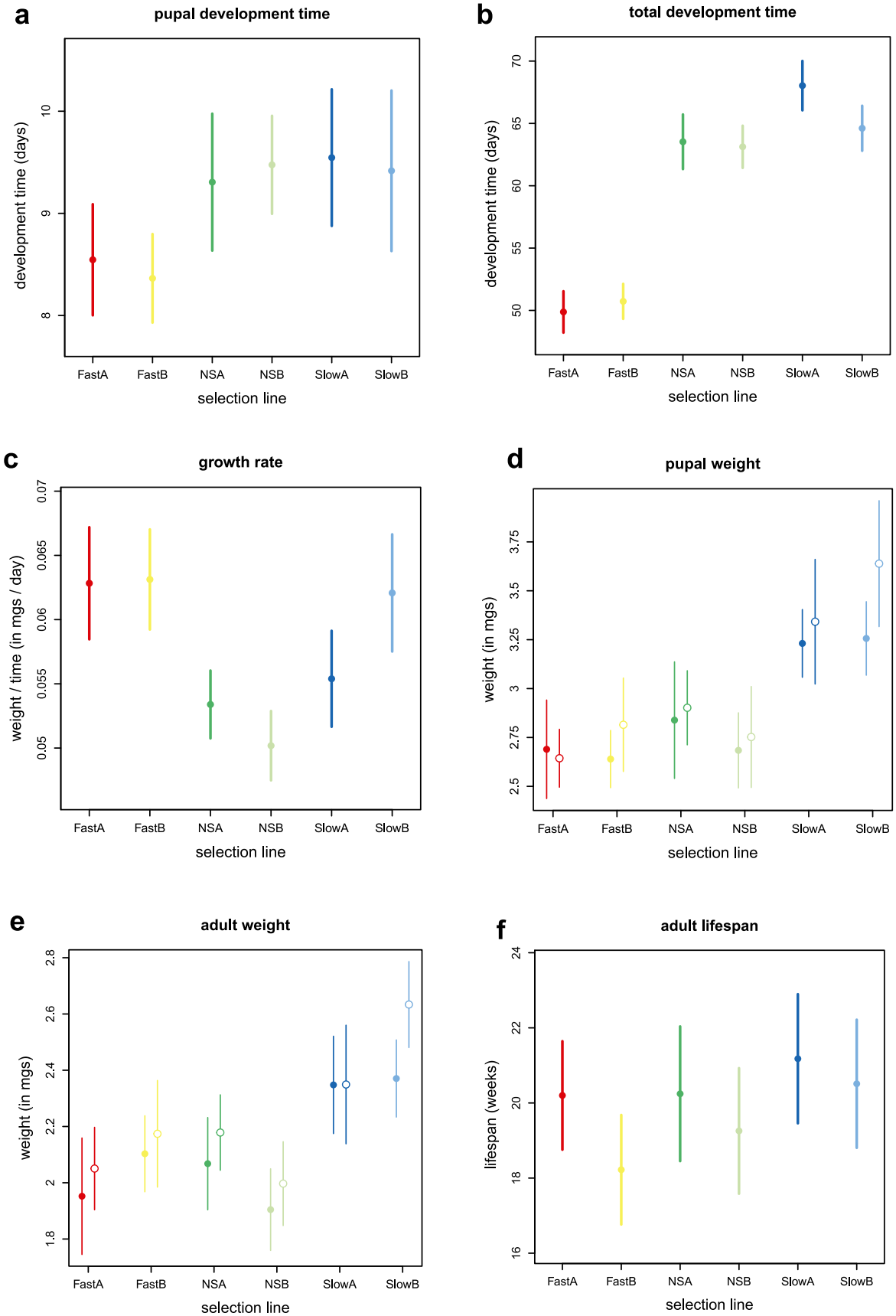

Extended Data Fig. 1 | See next page for caption.

https://doi.org/10.1038/s41559-023-02246-y

Extended Data Fig. 1 | Life history traits of the selection lines. (a) Pupal DT (days from pupation to eclosion; means ± 2 × s.e.m.) of the selection lines. Selection regime had an effect ($\chi^2 = 10.75$; df = 2; p = 0.046): pupae from the fast lines develop significantly faster than those of the non-selected lines ($\chi^2 = 8.13$; df = 1; p = 0.004). Sex had no effect ($\chi^2 = 0.017$; df = 1; p = 0.897). N = 48 for each selection line. b, Total postembryonic developmental time of the selection lines (days from hatching to eclosion; means ± 2 × s.e.m.). Selection regime had an effect ($\chi^2 = 22.98$; df = 2; p = 0.00001): fast lines develop significantly faster than the non-selected lines ($\chi^2 = 19.43$; df = 1; p = 0.00001). Sex had no effect ($\chi^2 = 0.2647$; df = 1; p = 0.61). N = 48 for each selection line. **(c)** Growth rate defined as adult weight (see e) divided by total postembryonic time (see b) of an individual (mg/day; means ± 2 x s.e.m.). Selection regime had an effect ($\chi^2 = 11.099$; df = 2; p = 0.0039), but the fast lines are not significantly different from the slow lines ($\chi^2 = 2.34$; df = 1; p = 0.127). Sex had no significant effect ($\chi^2 = 3.42$; df = 1; p = 0.065). N = 48 for each selection line. **(d)** Pupal weight in the selection lines (mg; means ± 2 x s.e.m). Sex had an effect; closed circles are male, open circles are female means ($\chi^2 = 4.24$; df = 1; p = 0.039). Selection regime also had an effect ($\chi^2 = 17.84$; df = 2; p = 0.00013): pupae from the slow lines are heavier than those of the non-selected lines ($\chi^2 = 13.09$; df = 1; p = 0.0003). N = 48 for each selection line. **(e)** Adult weight in the selection lines (mg; means ± 2 x s.e.m.). Sex had an effect ($\chi^2 = 6.04$; df = 1; p = 0.014), closed circles are male, open circles are female means. Selection regime also had an effect ($\chi^2 = 11.08$; df = 2; p = 0.039): adults of the slow lines are significantly heavier than adults of the non-selected lines ($\chi^2 = 7.78$; df = 1; p = 0.005). N = 48 for each selection line. **(f)** Life span in the selection lines (weeks as adult; means ± 2 × s.e.m). Selection regime had no effect ($\chi^2 = 4.6$, df = 2, p = 0.10). N = 90 for each selection line, see Methods.

https://doi.org/10.1038/s41559-023-02246-y

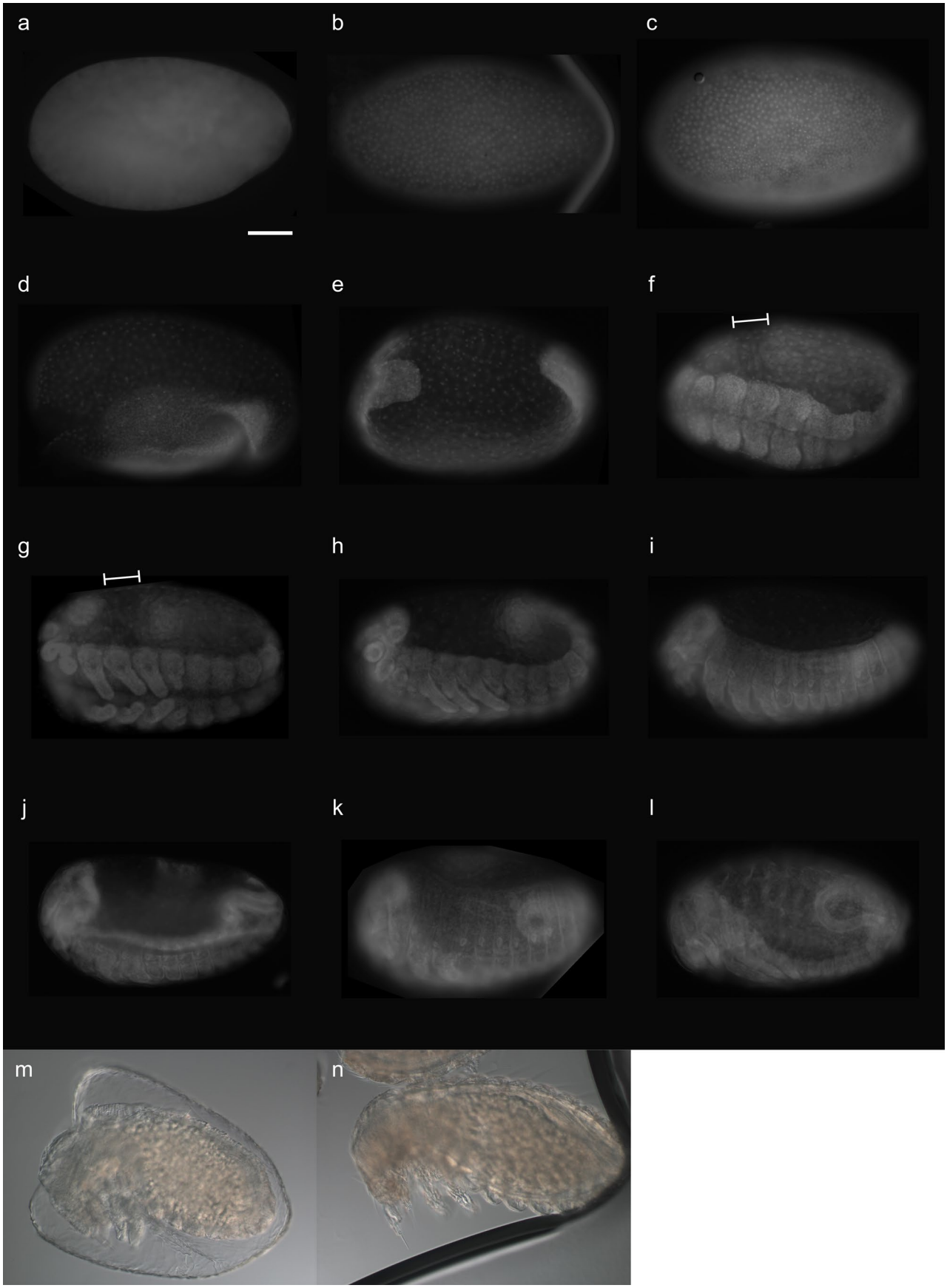

Extended Data Fig. 2 | See next page for caption.

https://doi.org/10.1038/s41559-023-02246-y

Extended Data Fig. 2 | Numerical staging table for *Tribolium castaneum*. Largely based on[93,94]. **(a)** 0 = no nuclei at surface; **(b)** 1 = undifferentiated blastoderm (equal nuclei at the surface). **(c)** 2 = differentiated blastoderm (the large polyploid nuclei of the serosa can be distinguished from the more dense, smaller nuclei of the germ rudiment). **(d)** 3 = gastrulation (amnion and serosa fold over the embryo; serosal window not yet closed). **(e)** 4 = extending germband (serosa closed). **(f)** 5 = extended germ band (distance between posterior end and head is small, size bar; limbs are buds). **(g)** 6 = limbs growing and extending (head and posterior of the germband still close, see size bar; limbs well developing and extending). **(h)** 7 = retracting germband (dorsal distance between head and posterior end of the embryo increases again). **(i)** 8 = completely retracted germband. **(j)** 9 = start of dorsal closure (rupture of the extraembryonic membranes, dorsal organ formation). **(k)** 10 = dorsal closure in progress (dorsal organ flatter, lateral sides of the embryo have moved towards dorsal). **(l)** 11 = dorsal closure completed (lateral sides of the embryo dorsally fused). **(m)** 12 = hatching (still in vitelline membrane). **(n)** 13 = hatched (out of vitelline membrane). Scalebar in (a) = 200 µm and applies to all panels.

https://doi.org/10.1038/s41559-023-02246-y

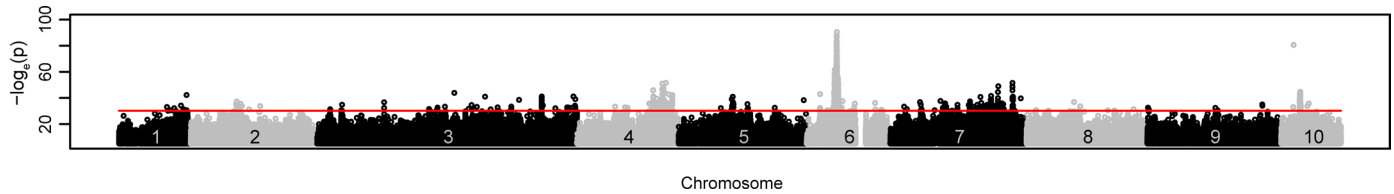

Extended Data Fig. 3 | Manhattan plot of SNPs that differ in allele frequency between the Slow and Non-Selected lines. P values of SNPs, based on a GLM contrasting the slow (n = 2) and the non-selected (n = 2) lines (see Methods), along the 10 chromosomes of *Tribolium castaneum*. In total, 1258 SNPs differ in frequency significantly (above the red line = $q < 0.01$, $-\log_e p > 33.0538$).

https://doi.org/10.1038/s41559-023-02246-y

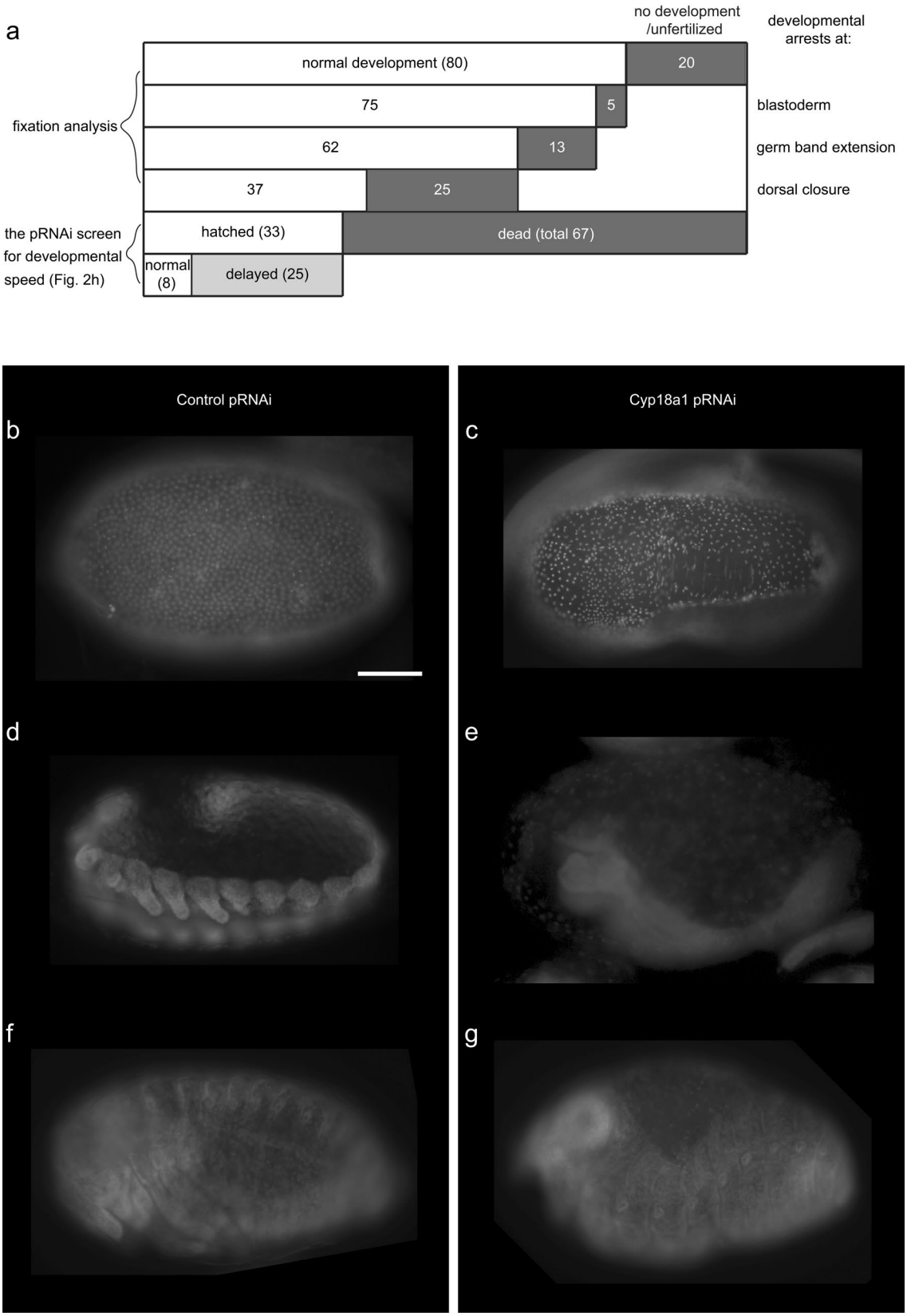

Extended Data Fig. 4 | See next page for caption.

https://doi.org/10.1038/s41559-023-02246-y

Extended Data Fig. 4 | Embryonic phenotypes upon *Cyp18a1* pRNAi. **(a)** Numbers (percentages) of the different phenotypic classes from one fixation analysis (upper 4 rows), in which *Cyp18a1* dsRNA injected mothers were allowed to lay eggs for one day, and batches of 25-50 eggs were fixed every subsequent day for DAPI staining and microscopic analysis. Percentages of developmental arrests are indicated with dark grey background, normal development with white background. The total number of developmental arrests corresponded well to the number of unhatched eggs after the pRNAi screen for developmental time (lower two rows). In 20% of the embryos, we did not observe any start of development at all (upper row), compared to 7.8% in the control RNAi. No developmental arrests were observed upon control pRNAi. **(b)** Control RNAi, normal blastoderm stage. **(c)** *Cyp18a1* RNAi. Developmental arrests at the blastoderm stage were recognized by irregular positioning of aberrant nuclei. **(d)** Control RNAi. Normal extending germband (fully extended in (d)). **(e)** Developmental arrests during germband extension were recognized by shortened and irregular germbands. **(f)** Control RNAi, normal dorsal closure. (**g**) *Cyp18a1* RNAi. Embryos that were arrested during dorsal closure were still open at the dorsal side, but showed otherwise advanced development. Scale bar in (b) = 200 µm and applies to panels b-g.

https://doi.org/10.1038/s41559-023-02246-y

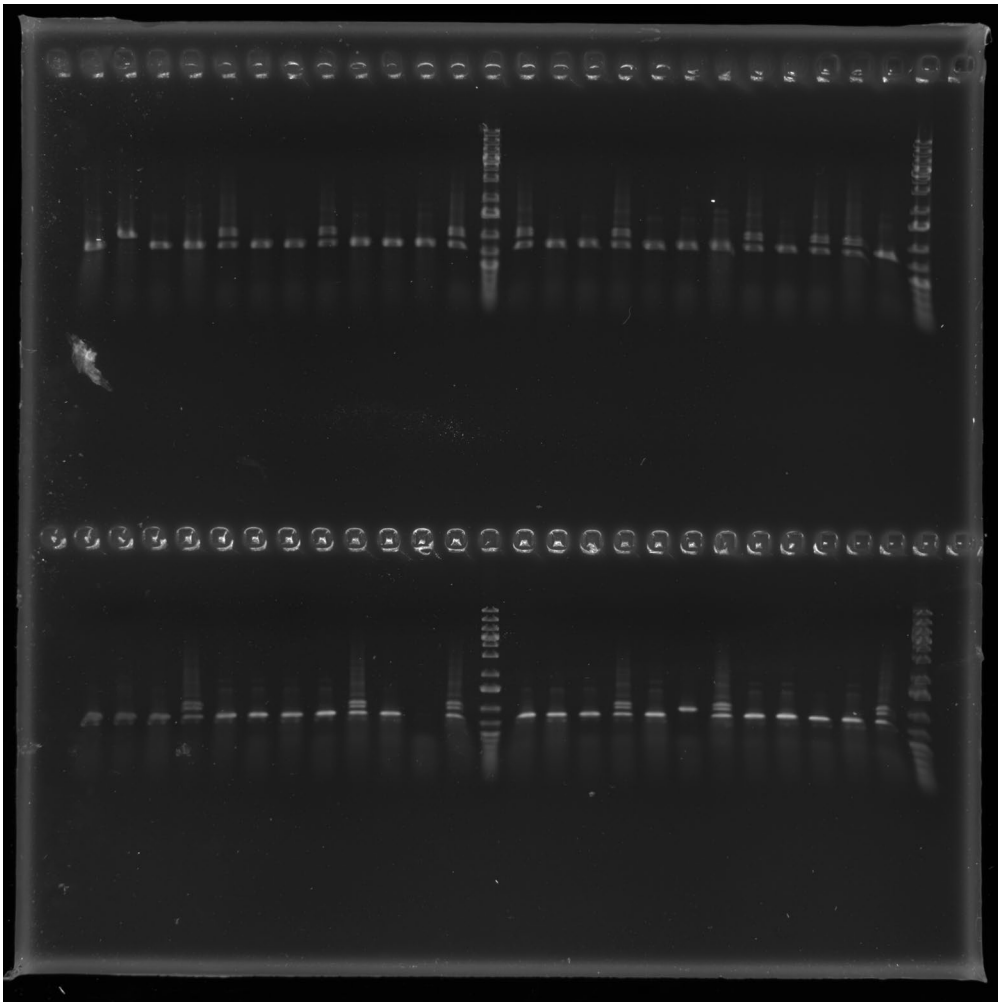

Extended Data Fig. 5 | Allele frequency of F in a natural population is 0.81. Genotyping PCR (Ethidium bromide staining shown on agarose gel) of one sample of 48 beetles from the (expanded) wild population collected by Rentokil from a bakery in The Netherlands (see Methods). 31 show only a 740 bp band (homozygous F allele), 2 show only a 942 bp band (homozygous S allele), and 14 are heterozygote (both bands + a hybrid band present). Thus the allele frequency of F is 0.81, and S is 0.19. Ladder is GeneRuler 1kb plus DNA ladder (Invitrogen).

nature portfolio

Corresponding author(s): Maurijn van der Zee

Last updated by author(s): Sep 14, 2023

Reporting Summary

Nature Portfolio wishes to improve the reproducibility of the work that we publish. This form provides structure for consistency and transparency in reporting. For further information on Nature Portfolio policies, see our Editorial Policies and the Editorial Policy Checklist.

Statistics

For all statistical analyses, confirm that the following items are present in the figure legend, table legend, main text, or Methods section.

n/a	Confirmed	
☐	☒	The exact sample size (*n*) for each experimental group/condition, given as a discrete number and unit of measurement
☐	☒	A statement on whether measurements were taken from distinct samples or whether the same sample was measured repeatedly
☐	☒	The statistical test(s) used AND whether they are one- or two-sided *Only common tests should be described solely by name; describe more complex techniques in the Methods section.*
☐	☒	A description of all covariates tested
☐	☒	A description of any assumptions or corrections, such as tests of normality and adjustment for multiple comparisons
☐	☒	A full description of the statistical parameters including central tendency (e.g. means) or other basic estimates (e.g. regression coefficient) AND variation (e.g. standard deviation) or associated estimates of uncertainty (e.g. confidence intervals)
☐	☒	For null hypothesis testing, the test statistic (e.g. *F*, *t*, *r*) with confidence intervals, effect sizes, degrees of freedom and *P* value noted *Give P values as exact values whenever suitable.*
☒	☐	For Bayesian analysis, information on the choice of priors and Markov chain Monte Carlo settings
☒	☐	For hierarchical and complex designs, identification of the appropriate level for tests and full reporting of outcomes
☒	☐	Estimates of effect sizes (e.g. Cohen's *d*, Pearson's *r*), indicating how they were calculated

Our web collection on statistics for biologists contains articles on many of the points above.

Software and code

Policy information about availability of computer code

Data collection	No software was used for data colection.
Data analysis	R (v3.6.1) including the coxme package (ref 74) and the vcfR package (v1.8.0, ref 81); Trimmomatic (v0.27, ref 75); BWA mem (v0-7-15, http://arxiv.org/abs/1303.3997); Samtools (v0.1.19, ref 76); Picard tools (v2.8.2, http://picard.sourceforge.net); GATK (v3.7-0, ref 77); varscan (v2.3.9, ref 78); snpEff (v.4.3, ref 79); IGV (v2.8.0, ref 88); BBduk (v 38.91, https://sourceforge.net/projects/bbmap/); SPAdes (v3.13.1, ref 89); FIMO (v5.5.4, ref 48). All custom made code is available at the Zenodo digital database http://doi.org/10.5281/zenodo.8395048

For manuscripts utilizing custom algorithms or software that are central to the research but not yet described in published literature, software must be made available to editors and reviewers. We strongly encourage code deposition in a community repository (e.g. GitHub). See the Nature Portfolio guidelines for submitting code & software for further information.

Data

Policy information about availability of data

All manuscripts must include a data availability statement. This statement should provide the following information, where applicable:

- Accession codes, unique identifiers, or web links for publicly available datasets
- A description of any restrictions on data availability
- For clinical datasets or third party data, please ensure that the statement adheres to our policy

Sequencing reads have been deposited in NCBIs Sequencing Read Archive as BioProject PRJNA942224. All other data are provided as supplementary data files. In this study, the Tcas 5.2 Tribolium genome sequence (ref 80), as well as the JASPAR database of binding matrices (ref 92) were used.

Research involving human participants, their data, or biological material

Policy information about studies with human participants or human data. See also policy information about sex, gender (identity/presentation), and sexual orientation and race, ethnicity and racism.

Reporting on sex and gender	n/a
Reporting on race, ethnicity, or other socially relevant groupings	n/a
Population characteristics	n/a
Recruitment	n/a
Ethics oversight	n/a

Note that full information on the approval of the study protocol must also be provided in the manuscript.

Field-specific reporting

Please select the one below that is the best fit for your research. If you are not sure, read the appropriate sections before making your selection.

☐ Life sciences ☐ Behavioural & social sciences ☒ Ecological, evolutionary & environmental sciences

For a reference copy of the document with all sections, see nature.com/documents/nr-reporting-summary-flat.pdf

Ecological, evolutionary & environmental sciences study design

All studies must disclose on these points even when the disclosure is negative.

Study description	From an outbred population (see Methods), we collected a 2h egg lay and selected the earliest-hatching half of the larvae for a fast line (FastA), and the latest-hatching half for a slow line (SlowA), and repeated this for two replicate lines (FastB, SlowB). We left two independent egg lays unselected
Research sample	Around 40 beetles were collected by athe commercial pest control agency Rentokil from a bakery in The Netherlands.
Sampling strategy	Random sampling
Data collection	standard laboratory procedurs, see methods
Timing and spatial scale	Start of artificial selection: 7 January 2013. End of artificial selection: 1 November 2017
Data exclusions	No outliers were detected or excluded.
Reproducibility	Number of replicates has been indicated.
Randomization	No groups were used
Blinding	No blinding was applied

Did the study involve field work? ☐ Yes ☒ No

Reporting for specific materials, systems and methods

We require information from authors about some types of materials, experimental systems and methods used in many studies. Here, indicate whether each material, system or method listed is relevant to your study. If you are not sure if a list item applies to your research, read the appropriate section before selecting a response.

Materials & experimental systems

n/a	Involved in the study
☒	☐ Antibodies
☒	☐ Eukaryotic cell lines
☒	☐ Palaeontology and archaeology
☐	☒ Animals and other organisms
☒	☐ Clinical data
☒	☐ Dual use research of concern
☒	☐ Plants

Methods

n/a	Involved in the study
☒	☐ ChIP-seq
☒	☐ Flow cytometry
☒	☐ MRI-based neuroimaging

Animals and other research organisms

Policy information about studies involving animals; ARRIVE guidelines recommended for reporting animal research, and Sex and Gender in Research

Laboratory animals	Tribolium castaneum (GA1 strain)
Wild animals	Adult Tribolium castaneum were collected using sieves and soft forceps, and sent to the laboratory in Falcon tubes containg flour by regular mail.
Reporting on sex	Effect of sex was tested
Field-collected samples	All populations were kept in Tupperware boxes containing wheat flour supplemented with 5% (w/w) dry yeast powder. Stock keeping and artificial selection were performed at 25°C, 65% relative humidity (RH), and 12/12h Light/Dark photoperiod in climate chambers. Populations are thus still mainatined in the laboratory.
Ethics oversight	For work with these invertebrate animals, no ethical approval is required. Transgenesis has been approved by the Dutch Health Authorites under permit GGO IG 21-118_2.8-000.

Note that full information on the approval of the study protocol must also be provided in the manuscript.